

Interreg
Greece-Italy
IR2MA

European Regional Development Fund



EUROPEAN UNION



University
Ioannina



HELLENIC REPUBLIC
REGION OF EPIRUS



ISTITUTO DI SCIENZE
DELLE PRODUZIONI
ALIMENTARI



CIHEAM
IAM BARI



CONSIGLIO
PER LA BONIFICA
DELLA CAPTANATA



Regione Puglia

Interreg V- A
Greece-Italy
Programme
2014 2020

www.greece-italy.eu

IR₂MA
Large Scale Irrigation
Management Tools for
Sustainable Water
Management in Rural
Areas and Protection
of Receiving Aquatic
Ecosystems

Subsidy Contract No: I1/2.3/27

WP#4

Deliverable 4.4.2

Results presentation

Project co-funded by
European Union, European Regional
Development Funds (E.R.D.F.) and by
National Funds of Greece and Italy

Front page back [intentionally left blank]

Interreg V- A Greece-Italy Programme 2014 2020

www.greece-italy.eu

Interreg
Greece-Italy
IR2MA

European Regional Development Fund



EUROPEAN UNION

IR₂MA

Large Scale Irrigation Management Tools for Sustainable Water Management in Rural Areas and Protection of Receiving Aquatic Ecosystems

Subsidy Contract No: I1/2.3/27

Partners



University
of
Ioannina



HELLENIC REPUBLIC
REGION OF EPIRUS



ISTITUTO DI SCIENZE
DELLE PRODUZIONI
ALIMENTARI



CIHEAM
IAM BARI



CONSORZIO
PER LA BONIFICA
DELLA CAPITANATA



Regione Puglia

PB1/LB UNIVERSITY OF IOANNINA - Research Committee (Uoi) <http://www.rc.uoi.gr/>

PB2 REGION of EPIRUS (ROE) <http://www.php.gov.gr/>

PB2 ISTITUTO SCIENZE DELLE PRODUZIONI ALIMENTARI (ISPA/CNR) <http://www.ispacnr.it/>

PB4 CIHEAM - ISTITUTO AGRONOMO MEDITERRANEO – BARI (IAMB) <http://www.iamb.it/>

PB5 CONSORZIO PER LA BONIFICA DELLA CAPITANATA (CBC) <http://consorzio.fg.it/>

Associated partners

REGION OF PUGLIA (ROP) <http://www.regione.puglia.it/>

Project co-funded by European Union, European Regional Development Funds (E.R.D.F.) and by National Funds of Greece and Italy

[illegible]

Deliverable 4.4.2 – Results presentation

Hydraulic Performance Analysis of On-Demand Pressurized Irrigation Systems in irrigation district 17 (Sinistra Ofanto)

Involved partners:

PB4 CIHEAM - ISTITUTO AGRONOMO MEDITERRANEO – BARI (IAMB)

PB5 CONSORZIO PER LA BONIFICA DELLA CAPITANATA (CBC)

Authoring team:

Andi Mehmeti	CIHEAM IAMB
Mladen Todorovic	CIHEAM IAMB

Contributors:

Anas Jarrar	CIHEAM IAMB
Nicola Lammadalena	CIHEAM IAMB
Vito Cantore	CNR-ISPA
Nicoletta Noviello	CBC

Place and time: Italy, 2020

IR₂MA

Project co-funded by European Union, European Regional Development Funds (E.R.D.F.) and by National Funds of Greece and Italy

Project co-funded by European Union, European Regional Development Funds (E.R.D.F.) and by National Funds of Greece and Italy



© This open-access document is published under the Creative Commons Attribution Non-Commercial ([CC BY-NC](https://creativecommons.org/licenses/by-nc/4.0/)) license and is freely accessible online to anyone.

Legal disclaimer

The sole responsibility for the content of this report lies with the authors. It does not represent the opinion of the European Communities. The European Commission is not responsible for any use that may be made of the information contained therein.

Table of content

Deliverable Information	1
Notes	4
Legal disclaimer	6
Figures	8
Summary	10
Riassunto	10
1. Introduction	11
2. Framework for performance assessment	12
3.1. Calculation of water requirement at the farm and hydrant level.....	14
3.2. GIS layout and hydrants	15
3.3. Hydraulic performance modeling	16
3. Results presentation	18
3.1 Hydraulic performance: Scenario 1, Freshwater irrigation.....	18
3.2 Hydraulic performance: Scenario 2, Network sectoring with freshwater and TWW sources. 27	
3.3 Applying deficit irrigation to improve the network performance	36
3.3.1 Performance analysis after deficit irrigation.....	37
4. Concluding remarks.....	48
References.....	49

Figures

Fig. 1. Summary of the methodology summarizing various calculation steps used in the study. ...	12
Fig. 2. The layout of Irrigation district 17.	13
Fig. 3. The number of hydrants within each sub-sector.	14
Fig. 4. The layout of the irrigation district, subsectors, and hydrant in GIS (Trinitapoli, Sinistra Ofanto).	16
Fig. 5. Seasonal Net Irrigation Requirement (NIR) for an average year.	18
Fig. 6. Indexed characteristic curves using 1000 random configurations. (a) Average year ($Q_{Clém} = 630$ L/s, $Z_0 = 67$ m a.s.l.); (b) dry year ($Q_{Clém} = 750$ L/s, $Z_0 = 67$ m a.s.l.).	19
Fig. 7. Pressure deficit curve of each hydrant (a), 100% pressure deficit curve (b) and 90% pressure deficit curve (c) for Average year ($Q_{Clém} = 630$ L/s, $Z_0 = 67$ m a.s.l) and dry year ($Q_{Clém} = 750$ L/s, $Z_0 = 67$ m a.s.l).	20
Fig. 8. Reliability curve regarding each hydrant generated using 1000 random configurations, and piezometric elevation $Z_0 = 67$ m a.s.l. a) average ($Q_{Clém} = 630$ L/s); b) dry year ($Q_{Clém} = 750$ L/s).	22
Fig. 9. GIS representation of 100% hydrant pressure deficit. a) average year ($Q_{Clém} = 630$ L/s, $Z_0 = 67$ m a.s.l), b) dry year ($Q_{Clém} = 750$ L/s, $Z_0 = 67$ m a.s.l).	24
Fig. 10. GIS representation of the 90% hydrant pressure deficit. a) average year ($Q_{Clém} = 630$ L/s, $Z_0 = 67$ m a.s.l); b) dry year ($Q_{Clém} = 750$ L/s, $Z_0 = 67$ m a.s.l).	25
Fig. 11. GIS representation of the reliability of each hydrant. a) average year ($Q_{Clém} = 630$ L/s, $Z_0 = 67$ m a.s.l); b) dry year ($Q_{Clém} = 750$ L/s, $Z_0 = 67$ m a.s.l).	26
Fig. 12. Indexed characteristic curves freshwater and TWW sectors (Climatic average year) generated using 1000 random configurations.	28
Fig. 13. Pressure deficit curve of each hydrant (a), 100% pressure deficit curve (b), and 90% pressure deficit curve (c) for sub-network 1 (freshwater) and sub-network 2 (TWW) using 1000 random configurations.	29
Fig. 14. Reliability curve for the sub-network 1 (freshwater) and sub-network 2 (TWW) using 1000 random configurations.	31
Fig. 15. GIS representation of the 100% pressure deficit of the sub-network 1 (freshwater) and sub-network 2 (TWW).	33
Fig. 16. GIS representation of 90% pressure deficit of the sub-network 1 (freshwater) and sub-network 2 (TWW).	34
Fig. 17. GIS representation of the reliability of each hydrant for sub-network 1 (freshwater) and sub-network 2 (TWW).	35
Fig. 18. Indexed characteristic curves for deciding to improve the system performance.	36
Fig. 19. Indexed characteristic curves for the average and dry year and sub-network 1 (freshwater) and sub-network 2 (TWW) generated by using 1000 random configurations.	38
Fig. 20. The 100% pressure deficit curves for the average and dry year and sub-network 1 (freshwater) and sub-network 2 (TWW) generated by using 1000 random configurations.	39
Fig. 21. GIS representation for 100% pressure deficit of each hydrant for sub-network 1. (a) Average year; (b) Dry year.	42
Fig. 22. GIS representation for 90% pressure deficit of each hydrant for sub-network 1. (a) Average year; (b) Dry year.	43
Fig. 23. GIS representation for the reliability of each hydrant for sub-network 1. (a) Average year (b) Dry year.	44
Fig. 24. GIS representation for 100% pressure deficit of each hydrant for sub-network 2. (a) Average year (b) Dry year.	45
Fig. 25. GIS representation for 90% pressure deficit of each hydrant for sub-network 2. (a) Average year (b) Dry year.	46
Fig. 26. GIS representation for the reliability of each hydrant for sub-network 2. (a) Average year (b) Dry year.	47

Tables

Table 1. Monthly average climatic attributes (Average year).....	14
Table 2. Input Crop characteristics in CROPWAT for CWR calculation.	15
Table 3. Operating data of the irrigation system, D17, Sinistra Ofanto.....	17
Table 4. Classes of relative pressure deficit and reliability with the associated color.....	17
Table 5. Monthly Net Irrigation Requirement (NIR) for an average year.	18
Table 6. The number and percentage of hydrants per each class of pressure deficit for the average and dry year, and both 100% and 90% pressure deficit.	21
Table 7. The number and percentage of hydrants per each class reliability (Average climatic year).	23
Table 8. The share of cropping pattern with fresh and treated wastewater.....	27
Table 9. The number and percentage of hydrants per 100% and 90% pressure deficit for sub-network 1 (freshwater) and sub-network 2 (TWW) using 1000 random configurations.	30
Table 10. The number and percentage of hydrants per each class reliability for the sub-network 1 (freshwater) and sub-network 2 (TWW).	32
Table 11. Irrigation percentage and a corresponding yield of each crop in two climatic years and two sub-networks.	37
Table 12. The number and percentage of hydrants per each class of pressure deficit for the average and dry year and sub-network 1 (freshwater) and sub-network 2 (TWW).	40
Table 13. The number and percentage of hydrants per each class of reliability for the average and dry year and sub-network 1 (freshwater) and sub-network 2 (TWW).	41

Summary

Hydraulic performance and sustainability are interlinked in large-scale irrigation schemes. Accordingly, auditing and assessing the hydraulic and water delivery performance of such schemes are needed for the proper operation. This study used the Crop Water and Irrigation Requirements Program of FAO (CROPWAT), geographic information system (GIS), and Combined Optimization and Performance Analysis Model (COPAM) to analyze the level of hydraulic (water delivery) performance providing useful information regarding the different operational options and level of performance. CROPWAT was used to simulate irrigation requirements for each crop based on soil, climate, and crop data for average and dry year conditions. GIS was used for the spatial distribution and visualization of the data. Finally, COPAM was used to assess the hydraulic performance of the irrigation system at the global and hydrant level under different operating conditions (upstream piezometric head Z and upstream discharge Q) and management practices (full or deficit irrigation). The performance analysis of this irrigation system with the use of simulation models was particularly useful to identify and quantify operation problems in the network sections for a wide range of possible operating conditions and the magnitude of these problems.

Keywords: irrigation service, performance assessment, COPAM, sustainability, hydraulic performance

Riassunto

Le prestazioni idrauliche e la sostenibilità sono interconnesse negli schemi di irrigazione su larga scala. Di conseguenza, la verifica e la valutazione delle prestazioni idrauliche e di erogazione dell'acqua di tali schemi sono necessarie per il corretto funzionamento. Questo studio ha utilizzato il Crop Water and Irrigation Requirements Program della FAO (CROPWAT), il sistema informativo geografico (GIS) e il Combined Optimization and Performance Analysis Model (COPAM) per analizzare il livello delle prestazioni idrauliche (fornitura di acqua) fornendo opzioni operative e livello di prestazioni. CROPWAT è stato utilizzato per simulare i requisiti di irrigazione per ciascuna coltura in base ai dati relativi al suolo, al clima e alle colture per condizioni di anno medio e secco. GIS è stato utilizzato per la distribuzione spaziale e la visualizzazione dei dati. Infine, COPAM è stato utilizzato per valutare le prestazioni idrauliche del sistema di irrigazione a livello globale e idrante in diverse condizioni operative (prevalenza piezometrica a monte Z e scarico a monte Q) e pratiche di gestione (irrigazione completa o deficitaria). L'analisi delle prestazioni di questo sistema di irrigazione con l'uso di modelli di simulazione è stata particolarmente utile per identificare e quantificare problemi di funzionamento nelle sezioni di rete per un'ampia gamma di possibili condizioni operative e l'entità di questi problemi.

Parole chiave: servizio di irrigazione, valutazione delle prestazioni, COPAM, sostenibilità, prestazioni idrauliche

1. Introduction

The Trinitapoli constitutes an important agricultural district and irrigation system, located within Ofanto River Basin, in the Apulia region. The district network is pressurized and was designed for on-demand operation allowing water delivery considering the time, duration, and frequency as defined by the farmers (Derardja et al., 2019). In the last decade cultivation of the more input demanding crops coupled with water-related hazards and climate change is leading to difficult water-efficient management practices and actual operating conditions of these systems which are different from those assumed at the design stage (Fouial et al., 2017). Hence, the performance of the water delivery network is worsening, the system suffers from inadequate discharge and pressure. Moreover, during peak periods, a restriction in water delivery is imposed (Levidow et al., 2014). Already today, groundwater resources in the region are being extracted at unsustainable rates triggering a multi-faceted crisis in terms of sustainability, quantity, quality, and management of water resources (Polemio, 2016). This, in turn, has increased the competition for water in the basin, and it is most probable that the water scarcity in the basin, particularly during the dry season, will be intensified in the years to come. Consequently, long-term integration of various conventional and non-conventional water management options must be considered. Agricultural wastewater reuse is experimentally implemented in the irrigation district 17 of Trinitapoli area for increasing water supply sustainability (D'Arcangelo, 2005).

Hydraulic performance and sustainability are interlinked in large-scale irrigation schemes (Dejen, 2011). The new sources of irrigation water and conditions of the water supply create concerns in terms of matching supply with demand, adequacy, equity, dependability, and efficiency of water distribution and delivery to various parts of the systems. Often, the variability of flow regimes in on-demand pressurized irrigation systems induces uncertainty in the pressure head at the hydrants affecting the system hydraulic performance and water delivery performance (Khadra et al., 2013). Discharges flowing in such networks strongly vary over time depending on the cropping pattern, the meteorological conditions, on-farm irrigation efficiency, and farmers' behavior, as well as on the number of hydrants simultaneously open (Lamaddalena and Lebdi, 2005). Models for analysis and performance criteria may contribute to support irrigation systems to operate satisfactorily within a wide range of possible demand scenarios (Lamaddalena and Sagardoy, 2000). The ultimate goals of managing irrigation water are efficiency, equity, and sustainability. Therefore, it is imperative to carry out detailed hydraulic analyses of the main water conveyance and distribution system considering different flow regimes in the design process for varying demand situations (Lamaddalena and Sagardoy, 2000).

This document led by PB4-CIHEAM-BARI provides the results of comparative spatial operational hydraulic and water delivery performance of district 17 (Trinitapoli) using geographic information system (GIS) and agro-hydrological and hydrodynamic simulation models. The study addressed current (business-as-usual) and re-engineering aspects of the existing irrigation delivery network under different operating scenarios (two sources of water) and management practices (full irrigation and deficit irrigation). The study made special emphasis on the hydraulic (water distribution) aspects of the performance, namely the *relative pressure deficit*, RPD, the *hydrant sensitivity*, RPDS, and the *hydrant reliability*, *R*. The results obtained generate useful results to suggest the most effective engineering and operational improvements.

2. Framework for performance assessment

A multi-step methodology was developed and applied with the intent of meeting the objectives of this study (Figure 1). Data collection included climate data, soil data, and crop data. The first part of the methodology entails the computation of irrigation requirements of the main crops grown in the district and each field of the irrigation district based on water, climatic, crop, and soil data using the CROPWAT 8.0 decision support tool. The second step included the creation of an ArcMap GIS-based network including agronomic, engineering, and network model data. GIS allows visualizing graphically, on maps previously digitized and geo-referenced, the critical zones of the system using different colors denoting the importance of the deficit in space and time.

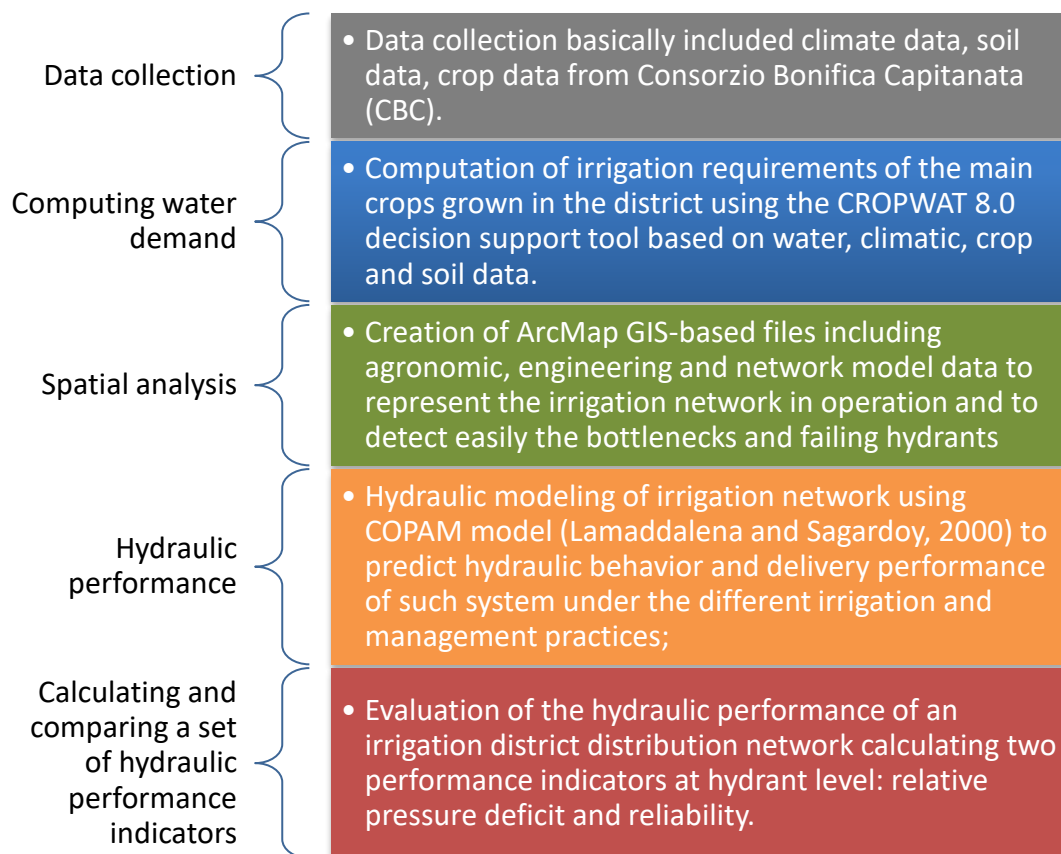


Fig. 1. Summary of the methodology summarizing various calculation steps used in the study.

Finally, the simulated demand flow configurations were used to the hydraulic simulation model Combined Optimization and Performance Analysis Model (COPAM) to simulate deliveries under different conditions and operational modes, analyze the network's hydraulic behavior, and evaluate hydraulic performance.

The performance was carried out for two scenarios:

I. Scenario 1: Business as usual

In this scenario, the performance was assessed under an average year and dry year climatic conditions, the cropping pattern for the whole district is assumed to be solely irrigated by surface water (freshwater).

II. Scenario 2: Adopting network sectoring and introducing wastewater

Testing the system performance considering that total area is shared between the two sources of water (freshwater and TWW), where each source contributes irrigating 50% of the total area. In district 17, there is a WWTP that is located in the surrounding of Trinitapoli with an average value of 300 m³/hr. as treatment capacity. The freshwater part is connected to the original freshwater source while the TWW is connected to the pumping station of a maximum discharge of 300 L/s and a pumping head of 6 bars.

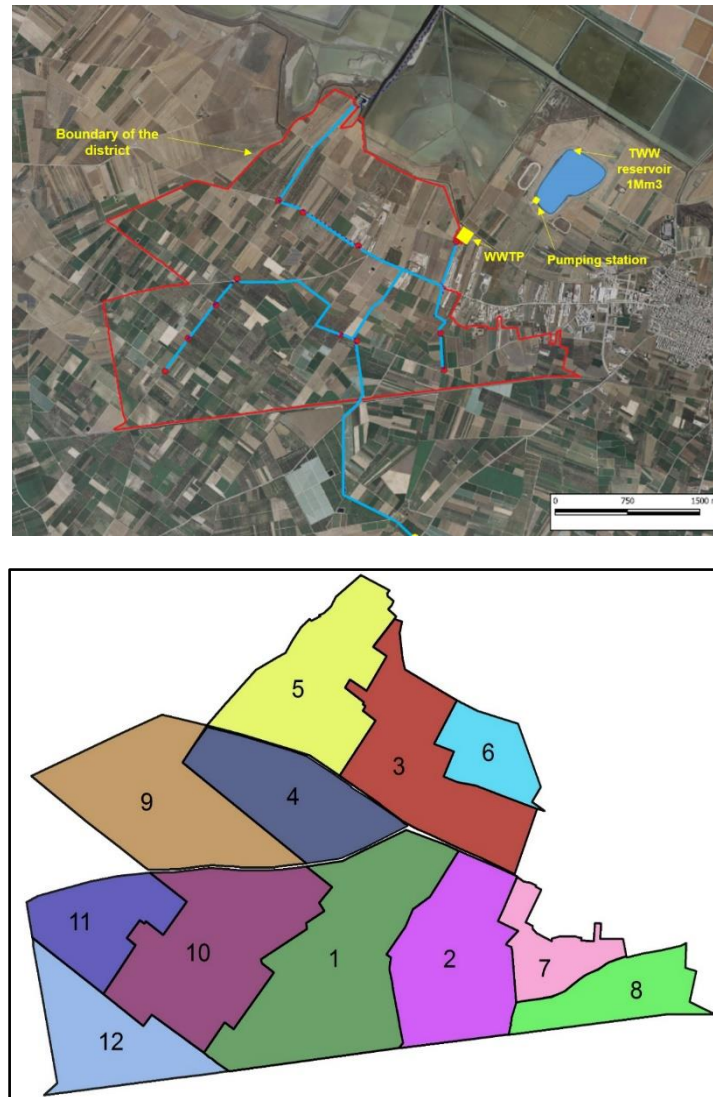


Fig. 2. The layout of Irrigation district 17.

The irrigation district 17 is divided into 12 sectors that represent the territorial units served by the irrigation distribution network and a network of irrigation facilities. The surface ranges from 20 ha to 300 ha. The irrigation district is served from 651 hydrants with a continuous flow rate of 0.202 l/s (reaching up to 0.303 l/s when operated 16/24) and minimum running pressure of 2 bars (20 meters). The number of hydrants in each sector is presented in Figure 3.

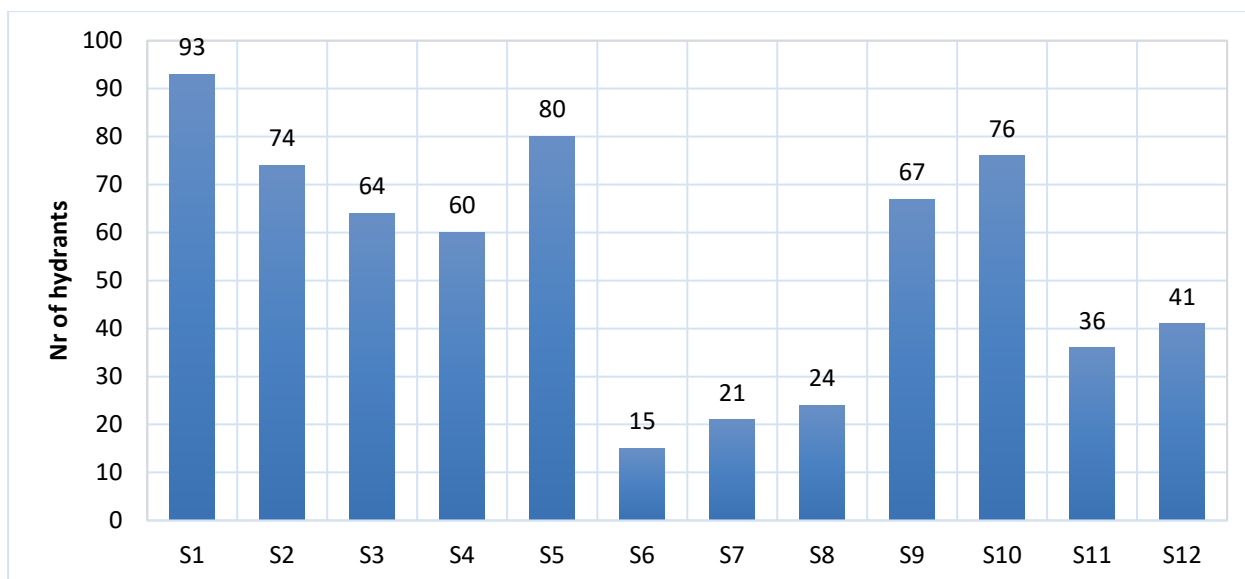


Fig. 3. The number of hydrants within each sub-sector.

3.1. Calculation of water requirement at the farm and hydrant level

Crop water requirements of the area served by the network were computed CROPWAT 8.0 decision support tool (Smith, 1992) based on climate, soil, and crop data. Table 1 shows monthly average climatic attributes (evaporation, rainfall, temperature, relative humidity, wind speed) for five years (2012 – 2016), obtained from "Finocchio" station (41°19'16.22" LN; 16°07'45.25" LE; Altitude, 16 m a.s.l.).

Table 1. Monthly average climatic attributes (Average year).

Month	Evaporation	Rainfall	Temperature (°C)			Relative Humidity (%)			Radiation	Wind
	(mm)	(mm)	Max	Min	Avg	Max	Min	Avg	cal/cm ² /d	km/d
Jan	15.8	39.1	12.5	3.1	7.3	97.1	62.0	83.4	160.0	79.7
Feb	24.9	51.2	13.2	3.7	8.1	97.4	62.8	83.7	218.0	98.2
Mar	49.1	57.6	16.1	5.7	10.7	97.0	57.4	80.5	328.4	111.1
Apr	78.7	45.0	20.3	8.7	14.3	94.7	49.7	74.5	453.1	107.8
May	110.3	40.0	24.0	11.7	17.9	93.5	45.3	70.1	543.7	110.1
Jun	136.7	31.2	28.9	16.0	22.5	89.3	42.9	66.1	622.1	95.3
Jul	151.0	10.6	32.1	18.7	25.3	88.4	39.6	64.3	618.1	91.7
Aug	131.2	29.9	31.7	18.7	24.8	92.4	43.2	69.0	548.9	92.7
Sep	77.2	75.9	26.8	15.0	20.3	97.8	52.6	79.9	397.8	76.9
Oct	40.5	41.3	22.2	11.6	16.2	99.6	65.8	88.6	259.3	60.7
Nov	20.5	89.0	18.1	8.2	12.5	98.9	68.6	88.7	177.3	74.9
Dec	13.1	33.9	13.5	3.5	7.6	98.9	66.4	88.6	152.2	80.6

Values of K_c, length of growing seasons for each crop as well as other crop characteristics (maximum root depth, critical depletion fraction, and yield response coefficient) necessary for irrigation scheduling are summarized in Table 2.

Table 2. Input Crop characteristics in CROPWAT for CWR calculation.

Crop	Kc_ini	Kc_mid	Kc_end	Planting	Stage_Ini (days)	Stage_Dev	Stage_Mid	Stage_Late	Stage_Tot	Root max	Critical depletion	Yield	Area
	-	-	-	-	days					M	-	-	ha
Olive	0.65	0.70	0.70	March	30	90	60	90	270	1.50	0.65	0.80	216.39
Wine grape	0.48	0.68	0.68	April	30	60	40	80	210	1.50	0.50	0.85	210.32
Autumn-winter cereals	0.70	1.15	0.25	Nov	30	140	40	30	240	1.50	0.55	1.05	117.00
Artichoke	0.50	1.00	0.95	Jul	40	40	220	30	330	0.90	0.45	1.00	78.73
Early Peach	0.50	0.90	0.70	Mar	30	60	120	30	240	1.50	0.50	1.10	57.72
Table grape	0.30	0.85	0.45	May	150	50	125	40	365	1.20	0.40	0.85	46.68
Apricot	0.53	0.86	0.73	Apr	30	60	120	30	240	1.50	0.50	1.10	28.24
Tomato	0.60	1.15	0.80	April	30	40	45	30	145	1.00	0.40	1.10	34.95
Almond	0.40	0.90	0.65	Mar	30	50	60	40	180	1.50	0.40	1.10	15.68
Late Peach	0.50	0.90	0.70	Apr	30	50	110	30	220	1.50	0.50	1.10	12.30
Melon	0.45	1.00	0.80	May	25	30	40	15	110	1.20	0.40	1.10	23.69
Mixed Orchard	0.50	0.90	0.80	Apr	30	50	70	30	180	1.50	0.60	1.10	8.70
Autumn vegetables	0.50	0.90	1.10	Oct	20	30	40	20	110	0.70	0.40	1.10	13.90
Spring vegetables	0.50	1.15	0.90	April	20	35	55	30	140	0.90	0.45	1.10	13.93

Net irrigation requirement (NIR) for the average year was used for the determination of optimal cropping pattern, while NIR for a dry year is applied for the calculation of the specific continuous discharge and the hydraulic parameters of the irrigation network. Specific continuous discharge (Eq. 1) represents the water demand of the optimal cropping pattern for the same period. It is defined as the discharge, if operated for 24 hours, would meet water need for one hectare of an average specific cropping pattern.

$$q_s \left(\frac{l}{ha} \right) = \frac{CWR \left(\frac{mm}{month} \right) \times 10 \left(\frac{\frac{m^3}{ha}}{month} \right) \times 1000 \left(\frac{L}{m^3} \right)}{30 (days) \times 24 (hr) \times 60 (min) \times 60 (sec)} \quad (1)$$

Computation of specific continuous discharge is a very significant step toward the implementation of the hydraulic performance assessment of the irrigation network under different scenarios.

3.2. GIS layout and hydrants

Using GIS (Geographical Information System), a layout of the distribution network for the study area was obtained, including the location of different hydrants along with the network. Figure 4 shows the developed general scheme of the irrigation network in ArcGIS map software. The developed GIS model allowed the visualization of the appropriate cropping pattern for the area under investigation computed irrigation requirements and corresponding irrigation water deficit or surplus, and facilitating the exploration of the results of such analyses. The physical configuration of the irrigation system included all the components that are needed to receive, convey, regulate, and measure the irrigation network from the source of the water to the user level. The network begins from a reservoir connected to a GFRP pipe of 700 mm diameter; this pipe comes from other districts, goes through the whole district, and supplies the water to all 12 sectors. It also continues supplying irrigation water to

other districts. Sectors, in turn, are linked to the main pipe by sector pipes through a head unit. A head unit is mounted at the head of the sector, it has many components to manage the sector, a flow meter, flow limiter, and a gate valve. The network which distributes the irrigation water to farms is installed downstream of the head unit and constructed by buried PVC pipelines that have diameters ranging from 100-250 mm. Irrigation water is delivered to farms throughout hydrants, where each one of these hydrants contains a gate valve, flow regulator, and flow meter. The irrigation area has 651 hydrants; each one has 10 L/s as nominal discharge.

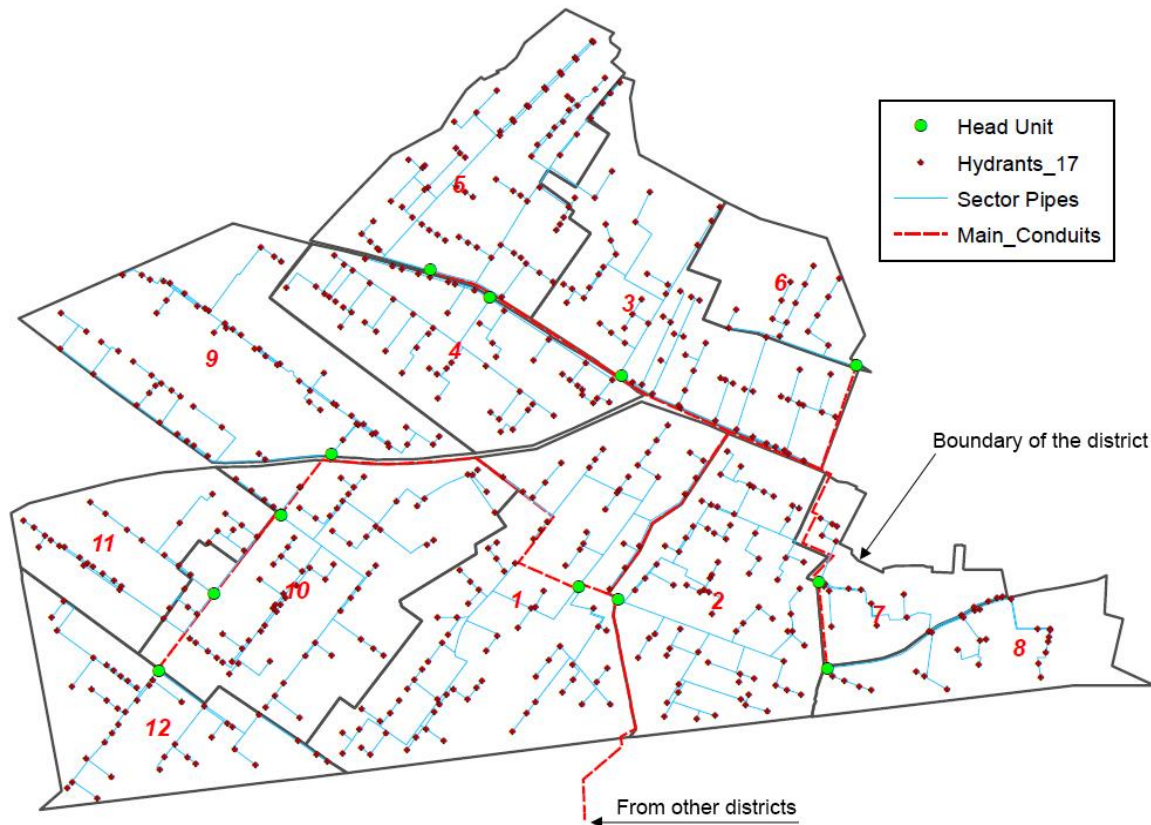


Fig. 4. The layout of the irrigation district, subsectors, and hydrant in GIS (Trinitapoli, Sinistra Ofanto).

Once the network map was generated and the cropping pattern was assigned, the water demand required to satisfy the irrigation needs of the present cropping pattern for each hydrant and area was computed for each hydrological year (NIR and GIR were estimated for both average and dry year).

3.3. Hydraulic performance modeling





The next steps consist of reproducing the hydraulic behavior and delivery performance of the system under different management practices. For this purpose, COPAM (Combined Optimization and Performance Analysis Model) software (Lamaddalena and Sagardoy, 2000) which analyzes the network's behavior and simulates hydraulic performance analysis of pressurized irrigation systems were used. Table 3 shows different parameters used in COPAM software to analyze the network performance.

Table 3. Operating data of the irrigation system, D17, Sinistra Ofanto.

Parameter	Value/description
Delivery schedule	On-Demand
Total area (ha)	920
Irrigated area (ha)	878
Specific continuous discharge for average climatic year (L/s/ha)	0.39
Clement's use coefficient	0.667
Minimum required head at each hydrant (m)	20
Available Clément discharge at the upstream end of the network (L/s)	330
Available piezometric head at the upstream end of the network (m)	6.7
Total number of hydrants	651
Nominal discharge of each hydrant (L/s)	10
Average area served by each hydrant (ha)	1.4
Minimum number of hydrants in simultaneous operation	4
Network reliability	95%, $U(P_q)=1.645$
The discharge of TWW pumping station (L/s)	300
Pressure head of TWW pumping station (bar)	6

The total area is 920 ha and the irrigated area 878 ha. The specific continuous discharge was 0.39 l/s/ha. The network consists of GFRP large and medium diameter pipes (400-700 mm) and PVC small diameters (100-250 mm) pipes that provide the water to farms. The roughness coefficient of these pipes, expressed in the unit Bazin coefficient γ ($m^{0.5}$), is equal to 0.06. For a better understanding of AKLA model outputs, the data was presented using GIS to give a spatial sense of the performance level. A color-coding was used to identify the hydrant according to its state (Table 4). The selected classes of pressure deficit (-5 to -1, -1 to -0.2, -0.2 to 0, and 0 to 5) are based on previous studies and simulations. Three (3) classes of reliability (<0.5, 0.5-0.8, and 0.8-1.0) were used to state the performance of each hydrant (Stamouli et al., 2017).

Table 4. Classes of relative pressure deficit and reliability with the associated color.

Class	Bad	Poor	Fair	Good
Relative pressure deficit	 (-5) to (-1)	 (-1) to (-0.2)	 (-0.2) to (0)	 (0) to (5)
Reliability	<0.5		0.5÷0.8	0.8÷1

3.Results presentation

The computed net irrigation requirement (NIR) was calculated for each crop on a monthly and seasonal basis. The synthesis of results is given in Table 5 and Figure 5.

Table 5. Monthly Net Irrigation Requirement (NIR) for an average year.

Crop	Jan	Feb	Mar	Apr	May	Jun	Jul	Aug	Sep	Oct	Nov	Dec
Olive	0	0	0	14.7	45.8	41.6	78.8	39.5	3.3	0	0	0
Wine grape	0	0	0	0	24.9	49.3	103.2	54.3	0.1	0	0	0
Autumn-winter cereals	0	0	5.8	53.7	109.5	50.1	0	0	0	0	0	8
Artichoke	0	0	4.1	42.6	91.9	78.8	78.8	49	13.9	0	0	11.5
Early Peach	0	0	0	15.5	75.4	94.2	142	91.2	16.4	0	0	0
Table grape	0	0	0	6.2	13.2	11	47.3	11.2	0	0	0	8.7
Apricot	0	0	0	9.8	54.9	83.5	142	91.2	16.4	0	0	0
Tomato	0	0	0	12.9	75.1	122.1	174.4	69.1	0	0	0	0
Almond	0	0	0	13.9	79.3	94.2	139.1	56.9	0	0	0	0
Late Peach	0	0	0	6.8	53.2	88.1	142	91.2	16.4	0	0	0
Melon	0	0	0	0	32.6	79.2	157.8	83.8	0	0	0	0
Mixed Orchard	0	0	0	7.8	55.6	83.7	142	91.2	16.4	0	0	8.4
Autumn vegetables	0	0	0	0	0	0	0	0	0	0	0	10.3
Spring vegetables	0	0	0	6.8	57.9	117.9	181	43.4	0	0	0	0

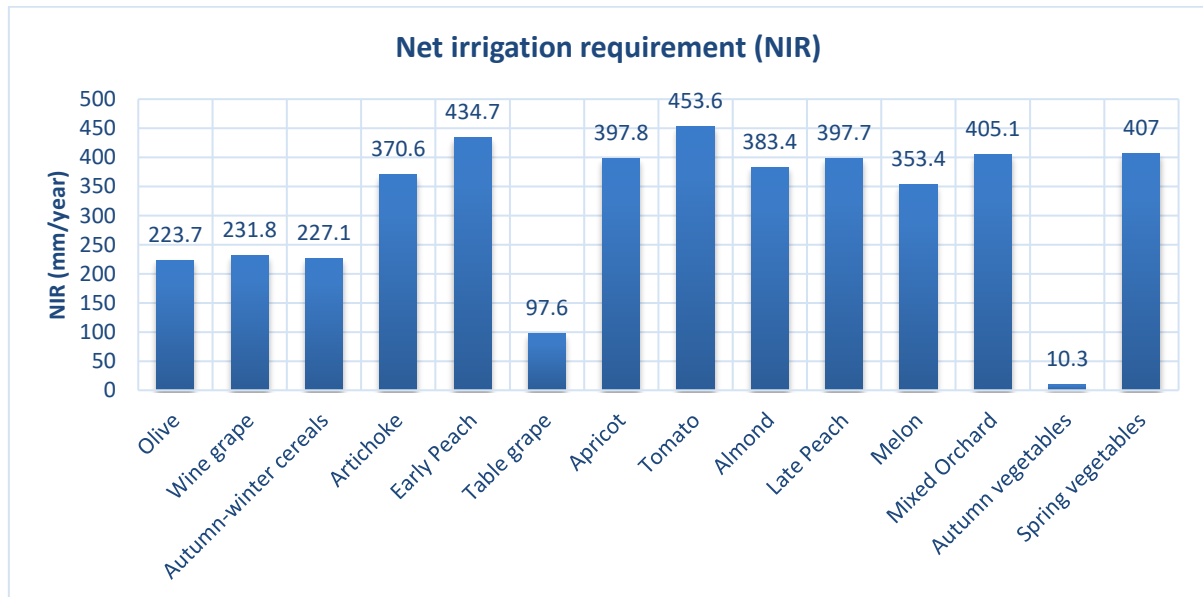


Fig. 5. Seasonal Net Irrigation Requirement (NIR) for an average year.

3.1 Hydraulic performance: Scenario 1, Freshwater irrigation

Figure 6 shows the indexed characteristic curves of the network for the average year using 1000 random configurations. As can be seen, the average year the set-point ($Q_{\text{clém}}=630$ L/s, $Z_{\text{opt}}=67$ m) shows a very low percentage of satisfied configurations, which is located outside the lower envelope of the indexed characteristic curves. As expected in the dry year, which is a dryer year, when locating

the setpoint ($Q_{clém}=750$ L/s, $Z_{opt}=67$ m) in indexed characteristic curves, the percentage of satisfied configurations goes lower than the average year, indicating a more critical level of network operation.

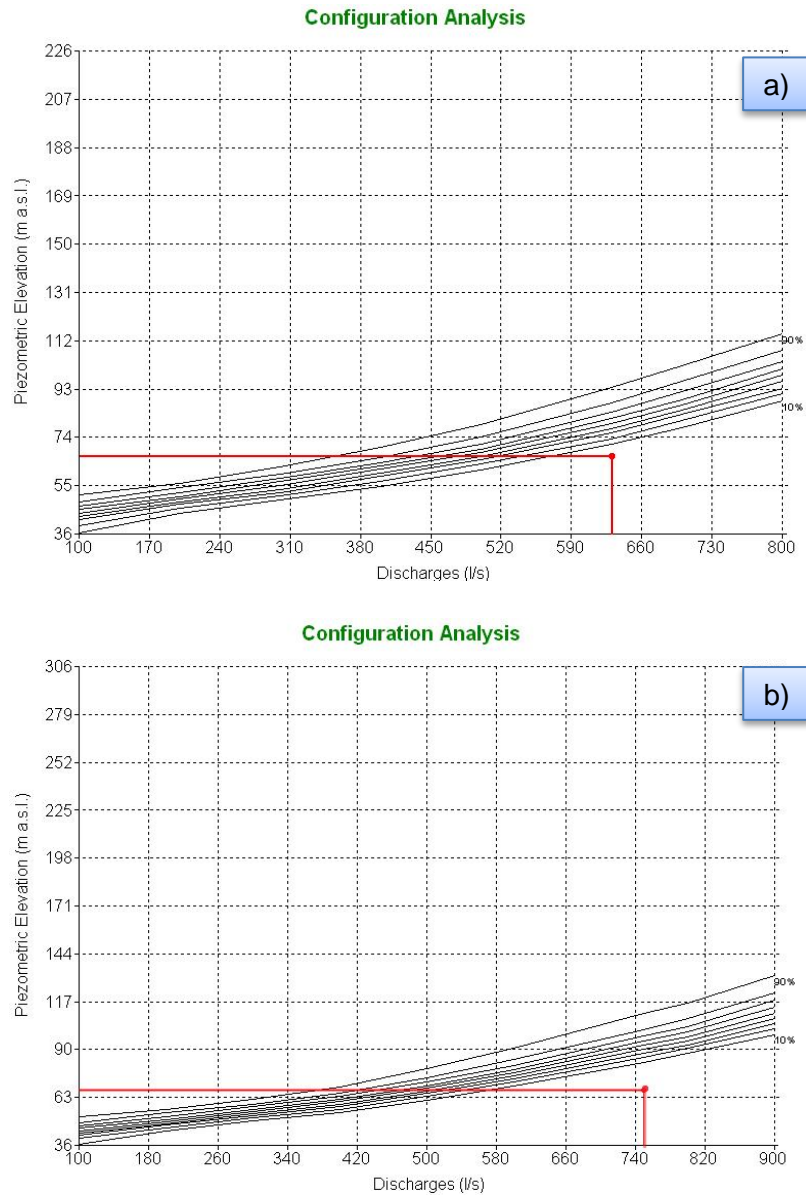


Fig. 6. Indexed characteristic curves using 1000 random configurations. (a) Average year ($Q_{clém} = 630$ L/s, $Z_0=of 67$ m a.s.l.); (b) dry year ($Q_{clém} = 750$ L/s, $Z_0=of 67$ m a.s.l.).

Figure 7 shows the performance indicators at the hydrant level, namely 100% pressure deficit, 90% pressure deficit (excluding 10% of unfavorable hydrants), and reliability regarding each hydrant when 1000 random configurations.

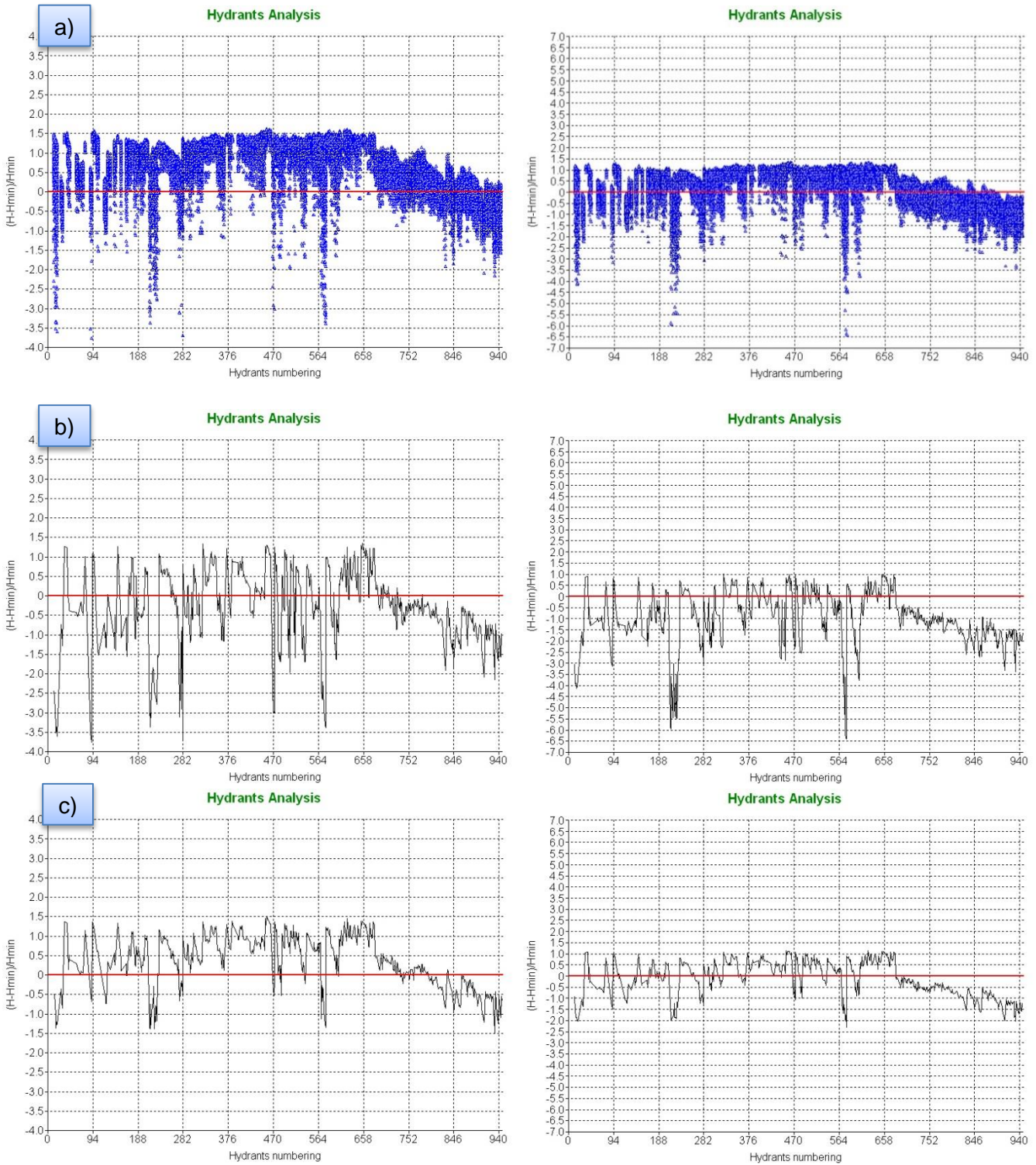






Fig. 7. Pressure deficit curve of each hydrant (a), 100% pressure deficit curve (b) and 90% pressure deficit curve (c) for Average year ($Q_{clém} = 630$ L/s, Z_0 =of 67 m a.s.l) and dry year ($Q_{clém} = 750$ L/s, Z_0 =of 67 m a.s.l).

Table 6 contains the number of hydrants per each class of pressure deficit and for both 100% and 90% pressure deficit. The table demonstrates the number of hydrants for each selected class and the corresponding hydrant percentage among the total number of hydrants. Table 6 and Figure 7 shows a low-pressure deficit is seen almost in all hydrants indicating very low network performance. In an average year, about 133 hydrants (21%) are under negative pressure when considering a 100% pressure deficit curve, while they drop to 23 (4%) in the case of a 90% pressure deficit curve. In the

poor pressure deficit class (-1) to (-0.2), there are 204 hydrants (32%) concerning 100 % pressure deficit curve, whereas it decreases to 108 hydrants (17%) when the 90% pressure deficit is taken into account. Likewise, reviewing the third class, namely (-0.2) to (0), the number of hydrants declines from 51 (8%) in the 100% pressure deficit curve to 47 (7%) in the 90% pressure deficit curve. Nevertheless, in the class (0) to (5) of pressure deficit, the number of hydrants increases from 240 (38%) in the 100% pressure deficit curve to 450 (72%) in the 90% pressure deficit curve. The drastic change in the system when switching between 100% and 90% pressure deficit, indicates a vulnerable system, where the vulnerability is defined as the magnitude of failure. Attention to such failure consequences should be paid, even though the probability of occurrence is low.

Table 6. The number and percentage of hydrants per each class of pressure deficit for the average and dry year, and both 100% and 90% pressure deficit.

Class	Bad	Poor	Fair	Good
				
Pressure deficit class	(-5) to (-1)	(-1) to (-0.2)	(-0.2) to (0)	(0) to (5)
Average Year				
100 % HPD	133	204	51	240
	21%	32%	8%	38%
90 % HPD	23	108	47	450
	4%	17%	7%	72%
Dry Year				
100 % HPD	288	150	24	155
	46%	24%	4%	25%
90 % HPD	101	193	52	282
	16%	31%	8%	45%

In the case of dry year and 100% pressure deficit, the table reveals that the number of hydrants included in pressure deficit classes bad (-5 to -1) increases from 133 (21%) in the average year to 288 (46%) in the dry year. Thus, the number of hydrants included in pressure deficit classes bad (-5 to -1) and poor (-1 to -0.2) increases from 337 (54%) in the average year to 438 (70%) in the dry year. On contrary, the number of hydrants included in pressure deficit classes fair (-0.2 to 0) and good (0 to 5) decreases from 291 (46%) in the average year to 179 (29%) in the dry year. The same trend happens when considering a 90% pressure deficit. The number of hydrants included in pressure deficit classes bad (-5 to -1) and poor (-1 to -0.2) from 131 (21%) in the average year to 294 (47%) in the dry year. Counter wise, the number of hydrants included in pressure deficit classes fair (-0.2 to 0) and good (0 to 5) decreases from 497 (79%) in the average year to 334 (53%) in the dry year. This situation indicates a lower performance of the system in the dry year when compared to the average year.

Figure 8 shows the reliability curve for each hydrant with 3 classes of reliability (<0.5, 0.5-0.8, and 0.8-1.0) were used to state the performance of each hydrant. According to Figure 8, there is a sufficient number of hydrants that have good reliability.

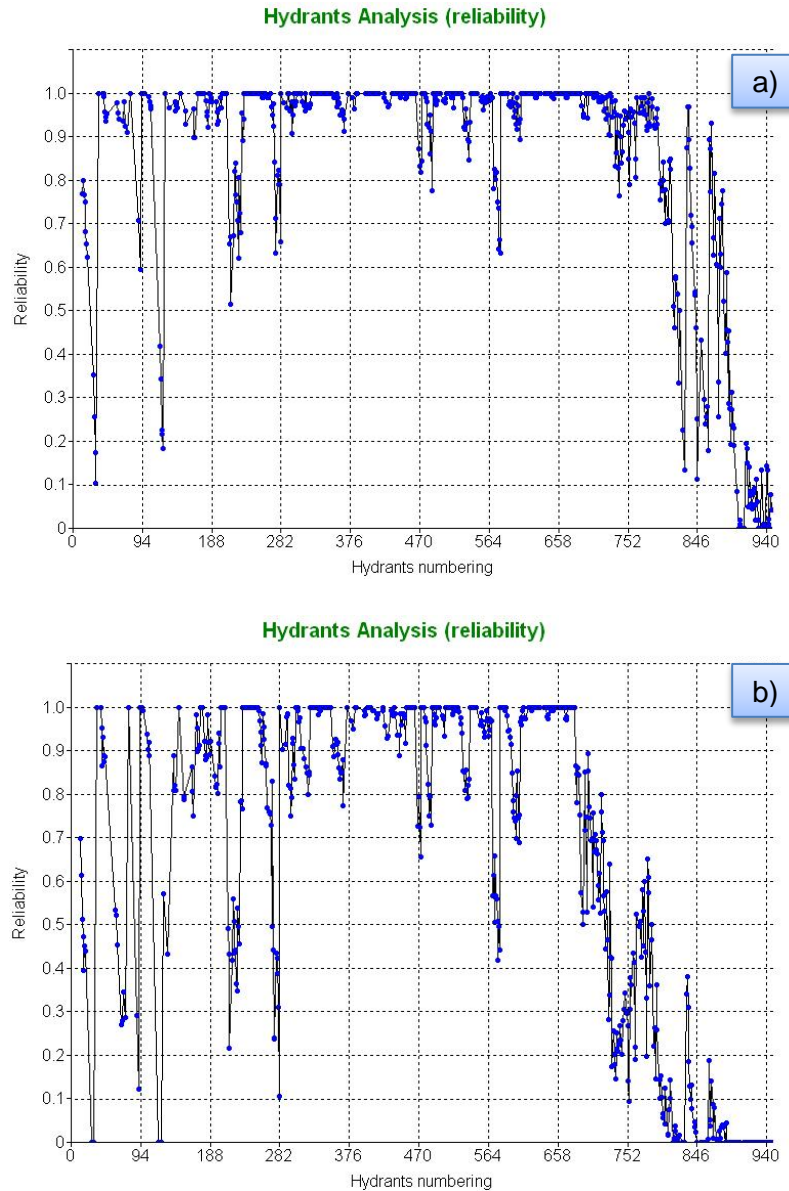


Fig. 8. Reliability curve regarding each hydrant generated using 1000 random configurations, and piezometric elevation Z_0 of 67 m a.s.l. a) average ($Q_{clém} = 630$ L/s); b) dry year ($Q_{clém} = 750$ L/s).

The number of hydrants per each class of reliability for the average year is reported in Table 7. From Table 7 about 73 hydrants (12%) have low reliability (<0.5), while there are 64 hydrants (10%) which have reliability between 0.5 and 0.8. However, the major number of hydrants, that is to say, 493 (79%), has an acceptable level of reliability (0.8-1.0). As mentioned before, the reliability is not enough to determine the level of hydrant performance. For instance, hydrant number 91 has very high reliability (0.94), but a very serious pressure deficit (-3.76). In the dry year, it is noticed that the number of hydrants that have reliability less than 0.5 increases from 73 (12%) to 197 (31%). However, for hydrant have reliability between 0.5 and 0.8, the number increased from 64 (10%) to 89 (14%). There is a reduction in the number of hydrants involved in the reliability class between 0.8 and 1.0, where the number decreases from 493 (79%) to 343 (55%). This variation of hydrant numbers points out a lower reliable system in the dry year comparing to the average year.

Table 7. The number and percentage of hydrants per each class reliability (Average climatic year).




Class	Reliability indicator		
	Bad	Fair	Good
Pressure deficit class			
	<0.5	0.5-0.8	0.8-1.0
100 % HPD	73	64	493
	12%	10%	79%
90 % HPD	197	89	343
	31%	14%	55%

Figure 9 shows the 100% pressure deficit of the hydrants represented in GIS. As shown, there are many hydrants subjected to vacuum pressure, and mainly distributed among sectors number 1, 2, 4, 5, 10, 11, 12. In such a situation, breaks may happen in pipelines and hydrants. The second class with yellow color (-1 to -0.2) is less dangerous, but still causing problems in pressure, resulting in inappropriate operation in the irrigation system. These hydrants extend through almost all the sectors except sectors 6 and 7. During the dry year, the hydrants undergo vacuum pressure which is distributed almost in all sectors except sectors number 6 and 7 pointing out for low operation performance. Figure 10 presents the 90% pressure deficit values (excluding the 10% of unfavorable hydrants) as represented using GIS. A considerable number of red color hydrants in 100% pressure deficit become either yellow, blue, or green, indicating the better performance of these hydrants. As mentioned before, this strong change in performance assigns for vulnerable systems. In this case, there is a 90% probability that the system attains performance as appears in Figure 10 and a 10% probability that it will exceed these values. The reliability of each hydrant is presented in Figure 11 using GIS. The figure shows that in an average year most of the hydrants are in green color, and have good reliability between 0.8 and 1.0, whereas few hydrants are in blue and red colors. This indicates that the system is reliable. However, reliability does not specify if the performance is good or not. It describes how many times the hydrant fails to meet the minimum required pressure among it all the appearance times in all configurations. The hydrants can be highly reliable but have a very low-pressure deficit. For example, some hydrants in sector 5 have good reliability, but at the same time, they have vacuum pressure. This means, these hydrants do not fail often, but once they fail, the failure is dangerous. In dry year hydrants having low reliability in red color (<0.5) are numerous, but mainly they are distributed in sectors 1, 9, 10, 11, and 12. Nevertheless, hydrants in blue colors (0.5-0.8) are few concentrated in sector 9. There is a good number of a hydrant in green color, which have reliability between 0.8 and 1.0. Comparing with normal year condition, the percentage of satisfied configurations change drastically, indicating the more critical level of network operation.

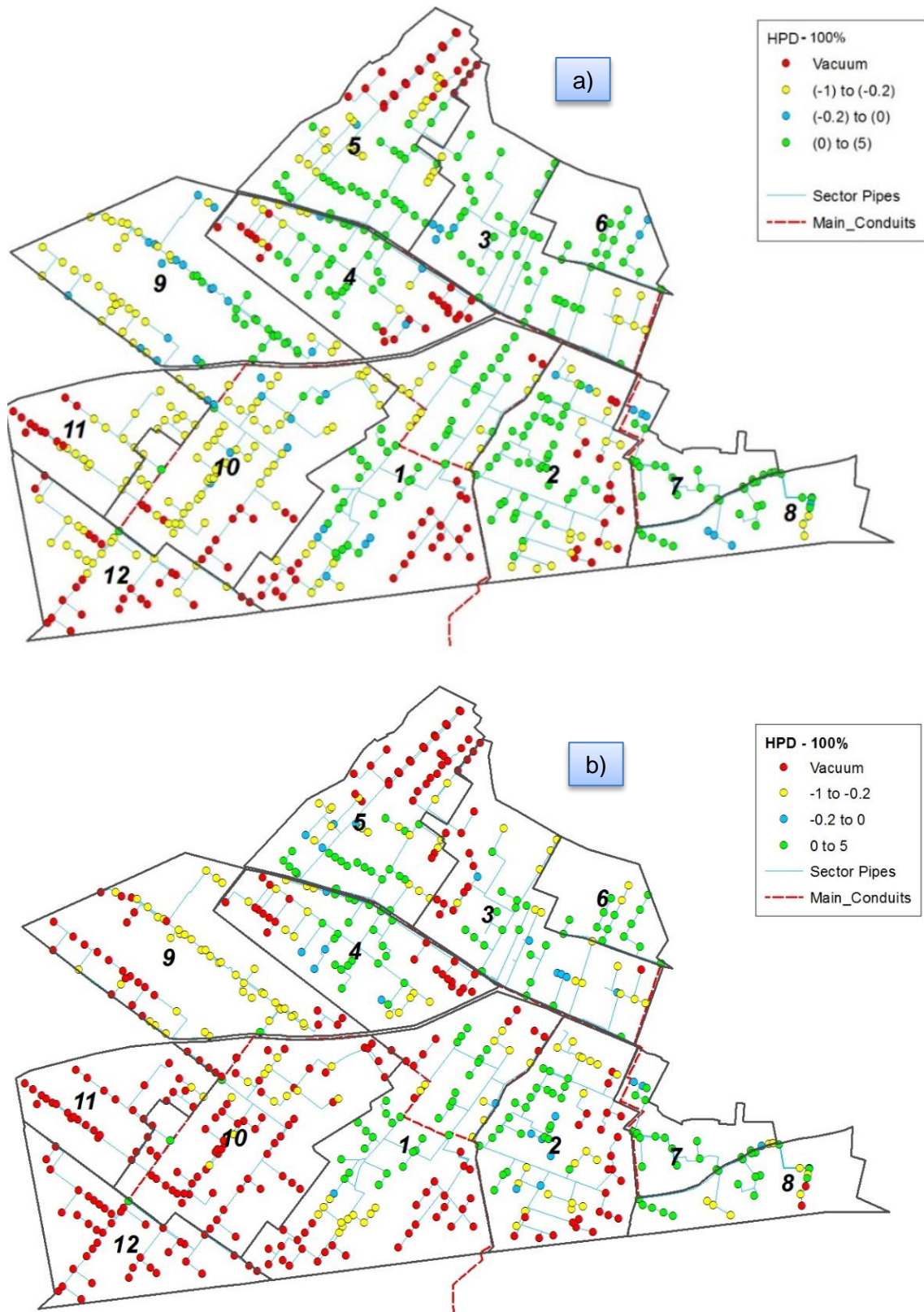


Fig. 9. GIS representation of 100% hydrant pressure deficit. a) average year ($Q_{clém} = 630 \text{ L/s}$, $Z_0 = 67 \text{ m a.s.l.}$), b) dry year ($Q_{clém} = 750 \text{ L/s}$, $Z_0 = 67 \text{ m a.s.l.}$).

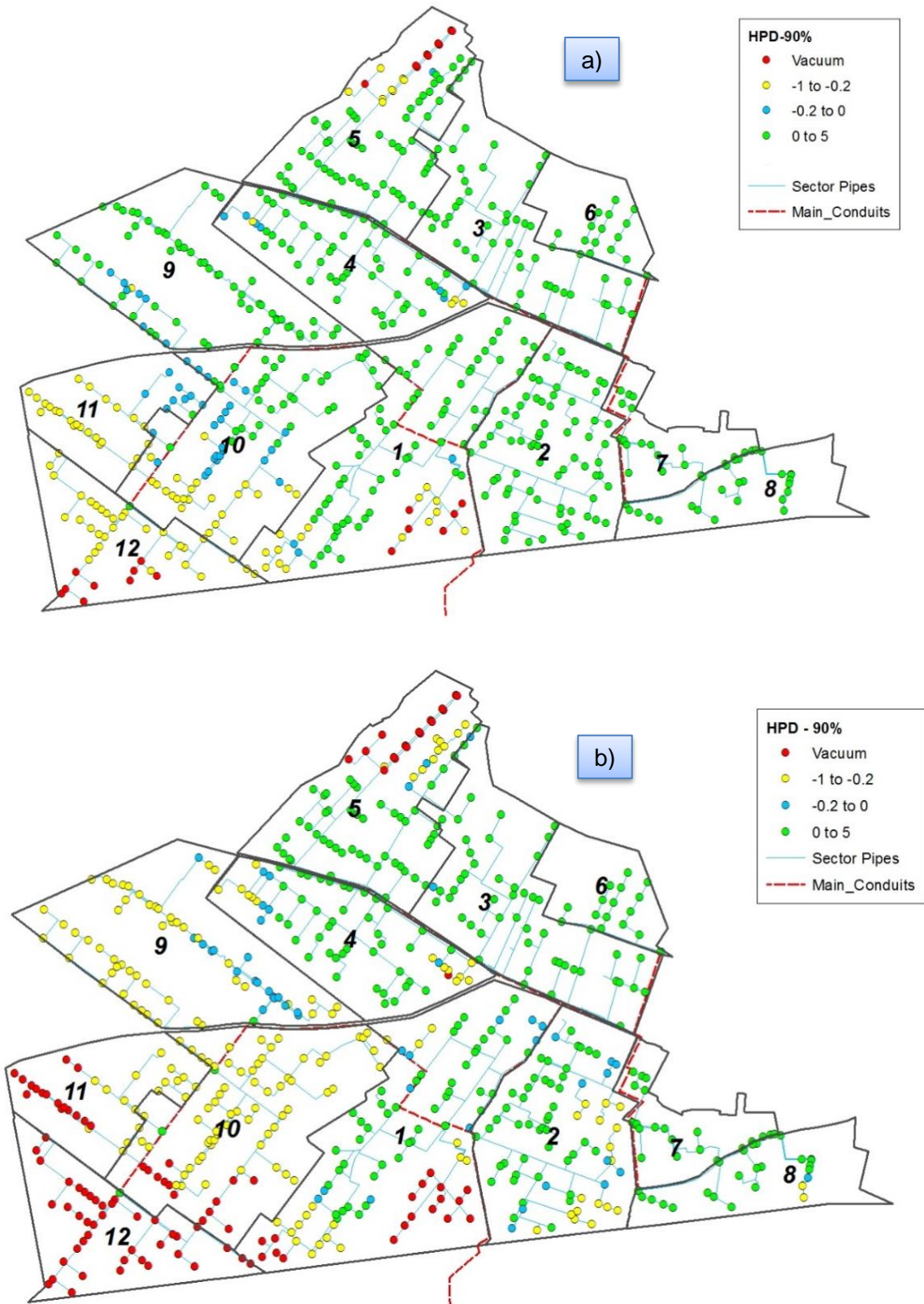


Fig. 10. GIS representation of the 90% hydrant pressure deficit. a) average year ($Q_{clém} = 630 \text{ L/s}$, $Z_0 = 67 \text{ m a.s.l.}$); b) dry year ($Q_{clém} = 750 \text{ L/s}$, $Z_0 = 67 \text{ m a.s.l.}$).

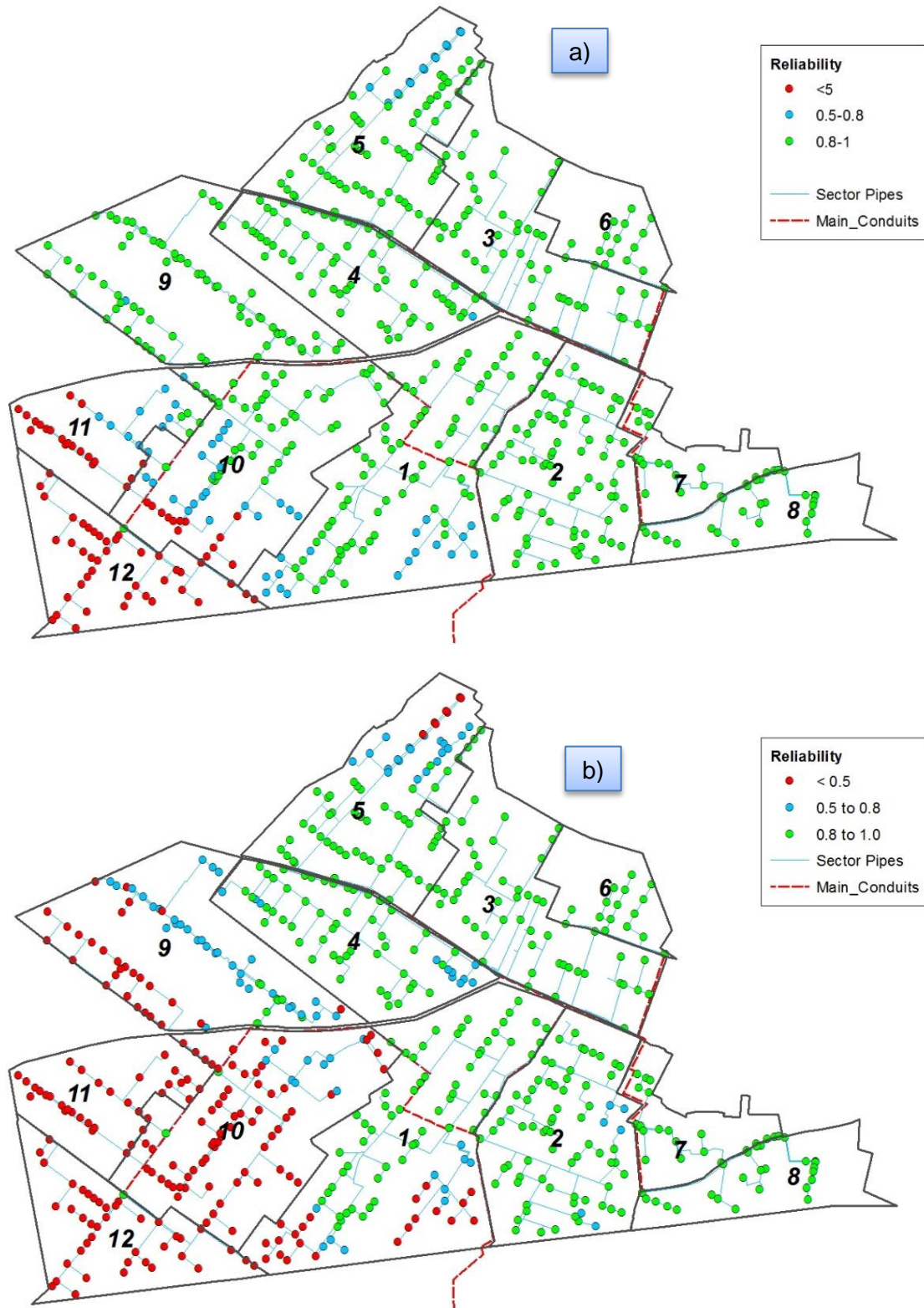


Fig. 11. GIS representation of the reliability of each hydrant. a) average year ($Q_{clém} = 630 \text{ L/s}$, Z_0 of 67 m a.s.l); b) dry year ($Q_{clém} = 750 \text{ L/s}$, Z_0 of 67 m a.s.l).

3.2 Hydraulic performance: Scenario 2, Network sectoring with freshwater and TWW sources.

In this scenario, the part irrigated by treated wastewater has an area of 452 ha including sectors 2,3,4,5,6,7 and 8, while the one irrigated by freshwater has an area of about 470 ha distributed among sectors 1, 9, 10, 11, and 12. Table 8 reports the crop pattern of the part irrigated from each source of water.

Table 8. The share of cropping pattern with fresh and treated wastewater.

Crop	Freshwater		Treated wastewater	
	Area (ha)	Area %	Area (ha)	Area %
Almond	-	-	14	3
Apricot	24	5	5	1
Artichoke	20	4	59	14
Autumn vegetables	4	1	10	2
Autumn-winter cereals	16	4	102	24
Early Peach	48	11	9	2
Late Peach	9	2	5	1
Melon	19	4	5	1
Mixed Orchard	3	1	5	1
Olive	128	28	89	21
Table grape	45	10	11	3
Tomato	14	3	23	5
Wine grape	124	27	88	21
Total	455 ha	100%	424	100

Figure 12 shows the indexed characteristic curves of the district parts irrigated by freshwater and TWW generated using the average climatic year. The set-point ($Q_{Clém}=330$ L/s, $Z_{opt}=67$ m) shows a very low percentage of satisfied configurations, which is located outside the lower envelope of the indexed characteristic curves. Figure 13 shows the performance indicators at the hydrant level, namely 100% pressure deficit, 90% pressure deficit (excluding 10% of unfavorable hydrants), and reliability regarding each hydrant when 1000 random configurations.

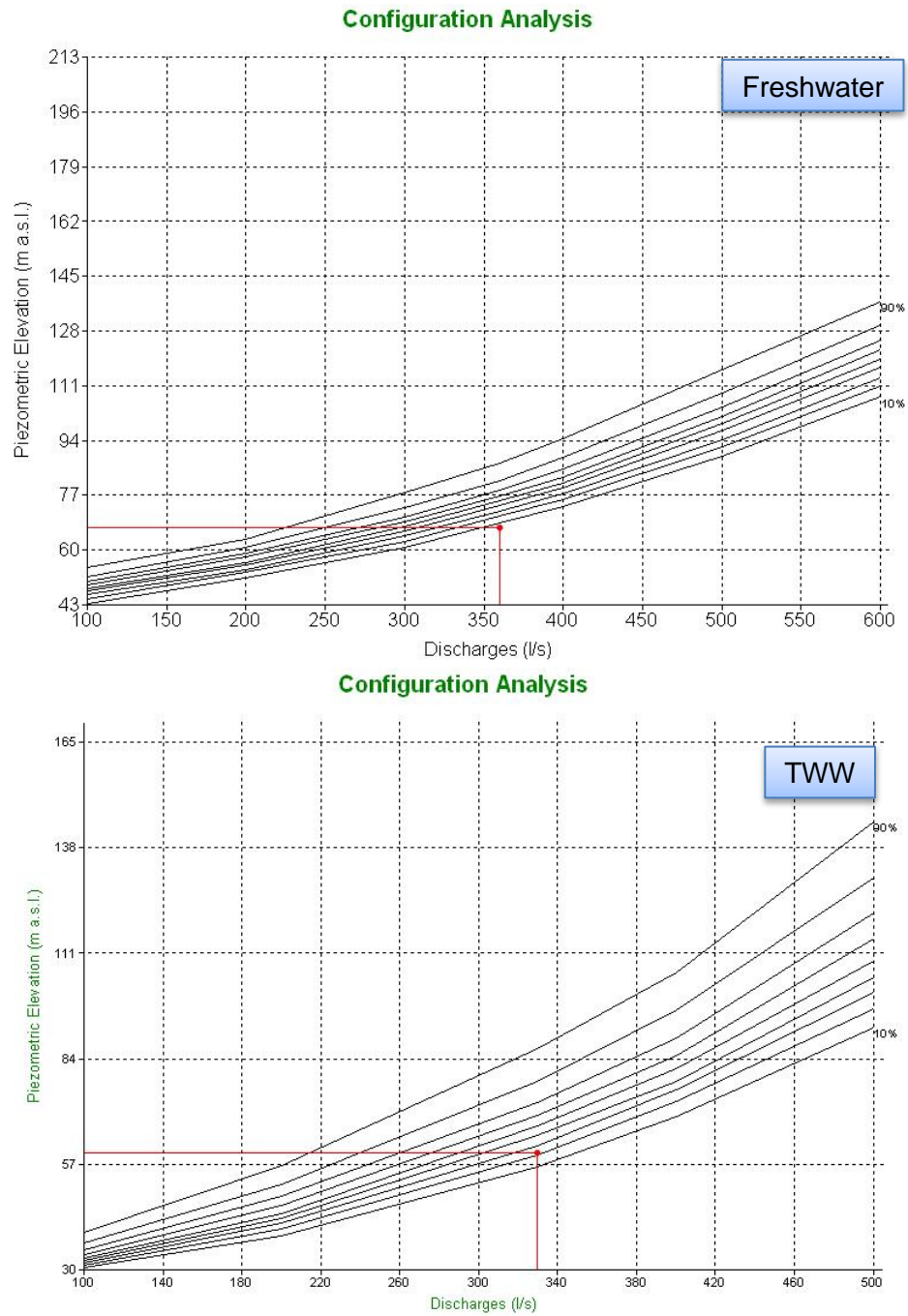


Fig. 12. Indexed characteristic curves freshwater and TWW sectors (Climatic average year) generated using 1000 random configurations.

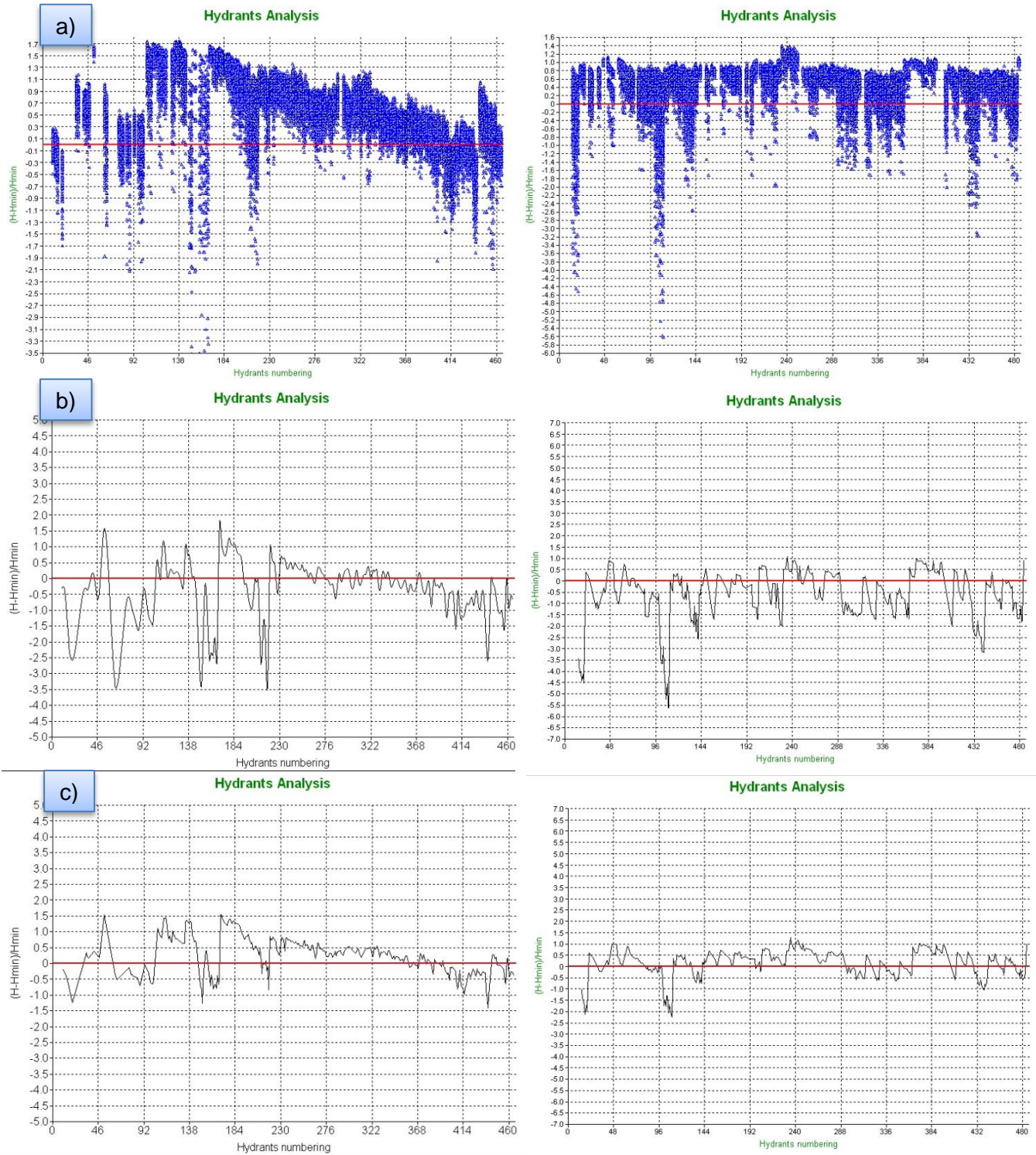






Fig. 13. Pressure deficit curve of each hydrant (a), 100% pressure deficit curve (b), and 90% pressure deficit curve (c) for sub-network 1 (freshwater) and sub-network 2 (TWW) using 1000 random configurations.

To analyze the situation in-depth, Table 9 reports the number and percentage of hydrants per each class of pressure deficit. For freshwater, regarding 100% pressure deficit, there are 51 hydrants (16%) are subject to negative pressure or bad class, which is a huge number, while there are 89 hydrants (29%) included in the poor pressure deficit class between -1 and -0.2. These hydrants also cause pressure problems for farmers. However, the fair pressure deficit class (-0.2 to 0) includes 45 hydrants (15%), whereas 125 hydrants (40%) are in good pressure deficit (0 to 5). Considering 90% pressure

deficit, the number of hydrants are 12 (4%) for bad pressure deficit class (-5 to -1), 69 (22%) for poor pressure deficit class between (-1 and -0.2), 21 (7%) for fair pressure deficit class (-0.2 and 0) and 208 (67%) for good pressure deficit class (0 and 5).

Table 9. The number and percentage of hydrants per 100% and 90% pressure deficit for sub-network 1 (freshwater) and sub-network 2 (TWW) using 1000 random configurations.

Class	Bad	Poor	Fair	Good
Pressure deficit class				
	(-5) to (-1)	(-1) to (-0.2)	(-0.2) to (0)	(0) to (5)
Sub-network 1 (freshwater)				
100 % HPD	51	89	45	125
	16%	29%	15%	40%
90 % HPD	12	69	21	208
	4%	22%	7%	67%
Sub-network 2 (TWW)				
100 % HPD	95	88	27	108
	31%	28%	9%	35%
90 % HPD	18	62	36	202
	6%	20%	12%	65%

For TWW there are 95 hydrants (31%) are exposed to negative pressure (-5 and -1). This percentage is high and confirms the low performance of the system. The high percentage (28%) of hydrants in the poor pressure deficit class between (-1 to -0.2) confirms the same results. The remaining part of hydrants is distributed among fair pressure deficit class -0.2 and 0 (9%) and 0 to 5 (35%). Keeping in view the 90% pressure deficit, the number of hydrants in the pressure deficit class between -5 to -1 is reduced from 95 hydrants (31%) to 18 (6%) when compared to 100% pressure deficit. Reduction in numbers of hydrants in the deficit class between -1 and -0.2 from 88 (28%) to 62 (20%) is noticed. Conversely, the number of hydrants in deficit class between -0.2 and 0 increases from 27 (9%) to 36 (12%) when compared to a 100% pressure deficit. Same trend in the positive deficit class (0 to 5), where the 108 hydrants (35%) increases to 202 (65%). A harsh change is noticed between the 100% and 90% pressure deficit indicating a vulnerable system.

According to Figure 14 and Table 10, for sub-network 1 there is a good number of reliable hydrants, but there are many hydrants with low reliability. In numbers, 40 hydrants (13%) have low reliability of less than 0.5. On the other hand, the hydrants with reliability from 0.5 to 0.8 are 45 (15%). Looking at good reliability hydrants in the reliability class from 0.8 to 1.0, there are 226 hydrants (73%). For sub-network 2 (TWW) the hydrants with low reliability (<0.5) are 5% in the system, while hydrants with reliability between 0.5 and 0.8 are 17%. A big percentage of the hydrants have reliability between 0.8 and 1.0.

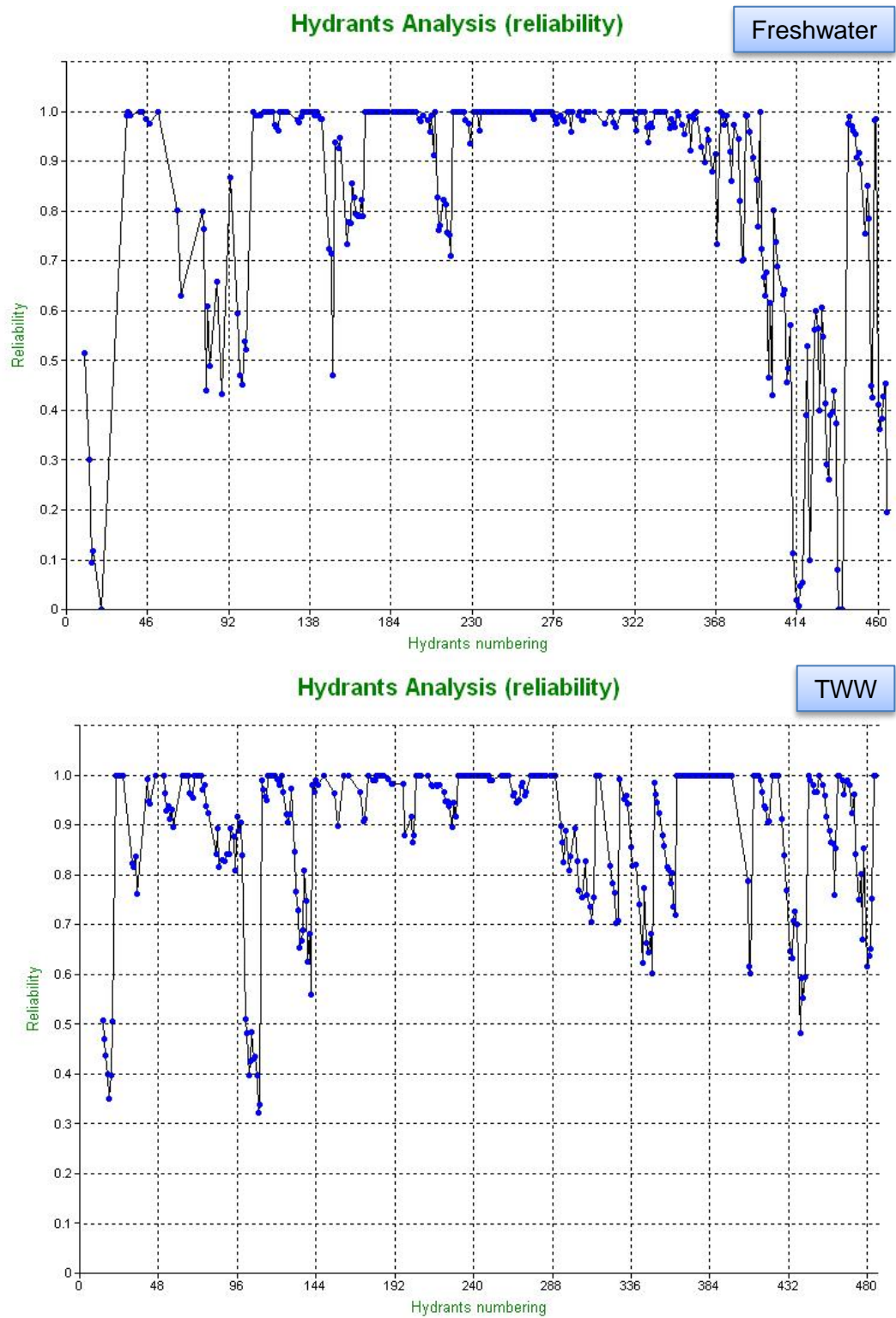


Fig. 14. Reliability curve for the sub-network 1 (freshwater) and sub-network 2 (TWW) using 1000 random configurations.

Table 10. The number and percentage of hydrants per each class reliability for the sub-network 1 (freshwater) and sub-network 2 (TWW).




Class	Realibility indicator		
	Bad	Fair	Good
Pressure deficit class			
	<0.5	0.5-0.8	0.8-1.0
Sub-network 1 (Freshwater)	40	45	226
	13%	15%	73%
Sub-network 2 (TWW)	197	89	343
	31%	14%	55%

Figure 15 shows the values of the 100% pressure deficit symbolized in GIS. For sub-network 1 (freshwater) the hydrants with bad performance (red color) are distributed in sectors 1, 10, 11, and 12. Hydrants with relatively poor performance (yellow color) are present in all sectors. In the 90% pressure deficit, most of the red hydrants turned green, yellow, or blue identifying a more stable system. Figure 15 indicates that hydrants of vacuum pressure are affecting the system performance for sub-network 2 (TWW), and they are present in sectors 2, 3, 4, 5, and 8. It is noticed also they are located in the area far from the pumping station at terminal points of the network. Additionally, hydrants with a pressure deficit of -1 to -0.2 (yellow color) are seen in almost all sectors. From Figure 16, negative pressure hydrants are reduced when contrasted with the 100% deficit values. Again, the probability that 90% pressure deficit vales will be exceeded is only 10%, but it happened, there will be a dangerous situation represented in Figure 15.



Fig. 15. GIS representation of the 100% pressure deficit of the sub-network 1 (freshwater) and sub-network 2 (TWW).

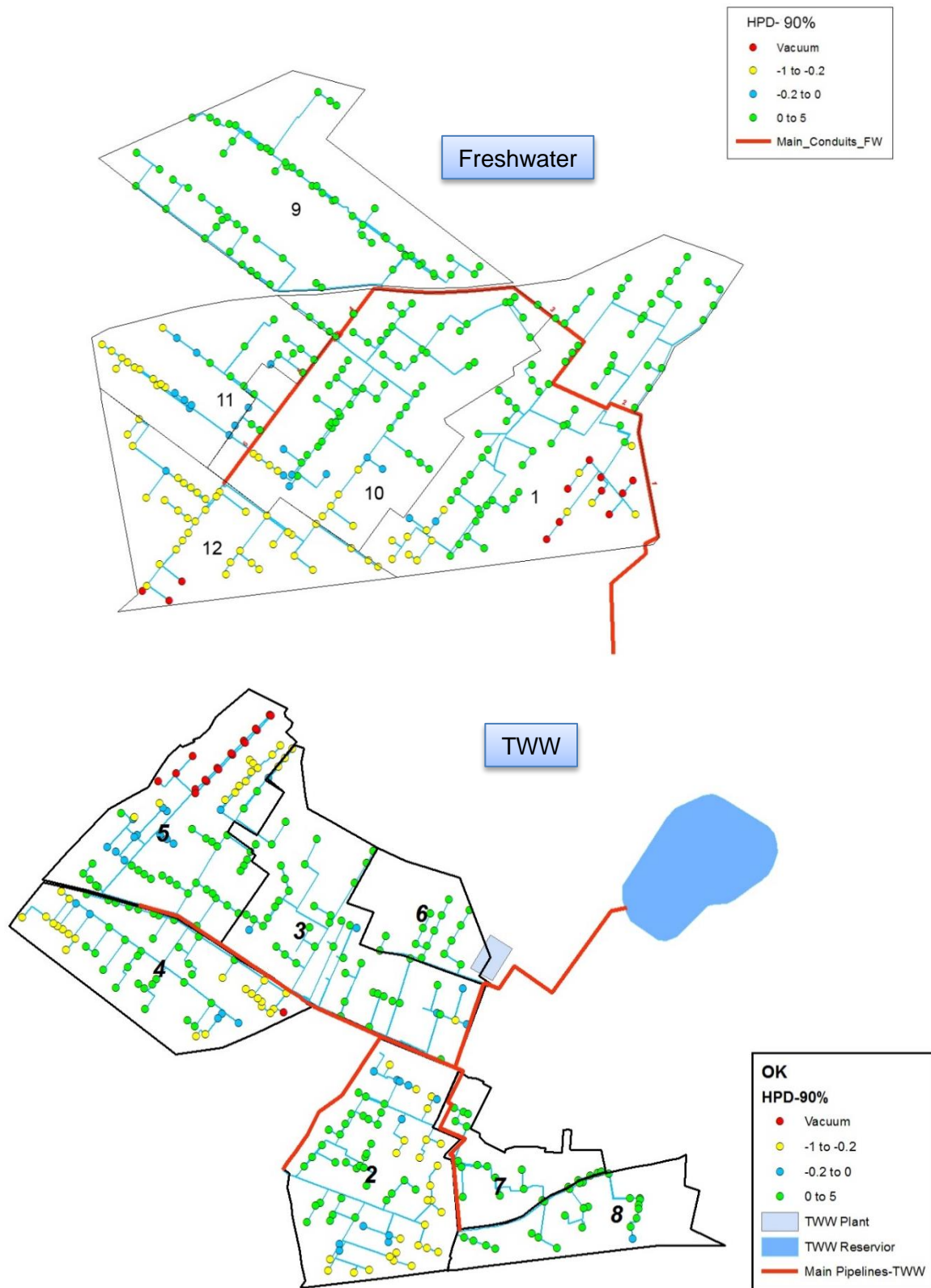


Fig. 16. GIS representation of 90% pressure deficit of the sub-network 1 (freshwater) and sub-network 2 (TWW).

The reliability of each hydrant is represented in Figure 17. For sub-network 1, hydrants with low reliability were detected for sector 12. For sub-network 2 (TWW), the green color is the prevalent color in almost all sectors, which indicates a reliable system except for some hydrants especially those

in red color in sector 5. Nevertheless, as mentioned before, the reliability itself is not enough to represent the system performance.



Fig. 17. GIS representation of the reliability of each hydrant for sub-network 1 (freshwater) and sub-network 2 (TWW).

3.3 Applying deficit irrigation to improve the network performance

Several steps can be done to enhance the percentage of satisfied configurations, thus, improve the network performance (Figure 18). The first step is to move the set-point up. This could be done by increasing the head of the pumping station. The second step is to decrease the demand discharge, where this step can be carried out by applying some management practices (e.g. applying deficit irrigation of crops). Step 3 is to stretch the envelope curves toward the set point. Practically this can be performed by changing the network characteristics (e.g. increasing a pipeline diameter downstream of the critical hydrants)

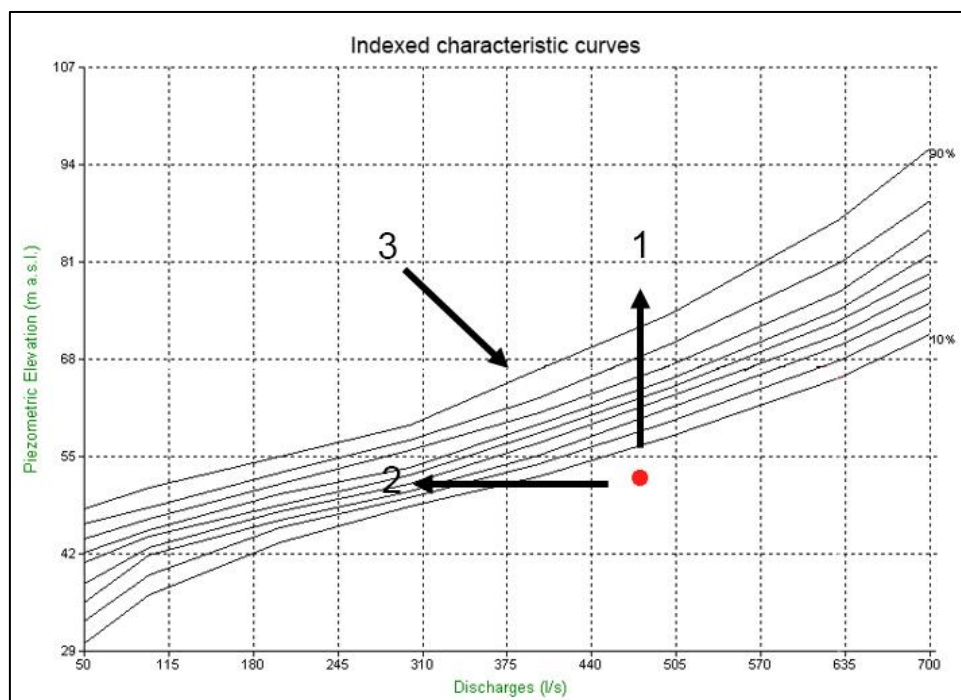


Fig. 18. Indexed characteristic curves for deciding to improve the system performance.

In this study, step number 3 has been followed to improve the system performance, which is to reduce the discharge by applying deficit irrigation for the cropping pattern. Table 11 shows the irrigation percentage of each crop and the corresponding yield for the average climatic year and the dry year. The resulted specific continuous discharge and the relating clement discharge are reported in the table as well.

Table 11. Irrigation percentage and a corresponding yield of each crop in two climatic years and two sub-networks.

Crop/parameter		Sub-network 1			Sub-network 2	
		Avg. year	Dry Year		Avg. year	Dry Year
q_s (L/s/ha)	Irrigation %	0.2	0.22	Irrigation %	0.195	0.234
$Q_{Clém}$ (L/s)		200	220		180	210
Crop		Yield %	Yield %			
Almond	0	0	0	65	93	90
Apricot	60	90	92	65	96	90
Artichoke	45	91	93	50	95	91
Autumn vegetables	20	100	100	20	100	100
Cereals	20	96	93	20	97	91
Early Peach	60	92	93	65	98	91
Late Peach	65	92	95	65	95	91
Melon	80	90	94	80	93	93
Mixed Orchard	60	89	93	65	94	92
Olive	25	92	90	30	95	90
Table grape	10	95	91	85	93	91
Tomato	85	92	97	80	93	90
Wine grape	0.50	89	90	55	94	90

3.3.1 Performance analysis after deficit irrigation

Figure 19 shows the indexed characteristic curves after applying the deficit irrigation. As noticed, a shift improvement happens when applying deficit irrigation. Considering the set-point ($Q_{Clém}=200$ L/s, $Z_{opt}=67$ m) of the average year, the percentage of the satisfied configuration of the system is above 90%. The same situation happens when considering the dry year.

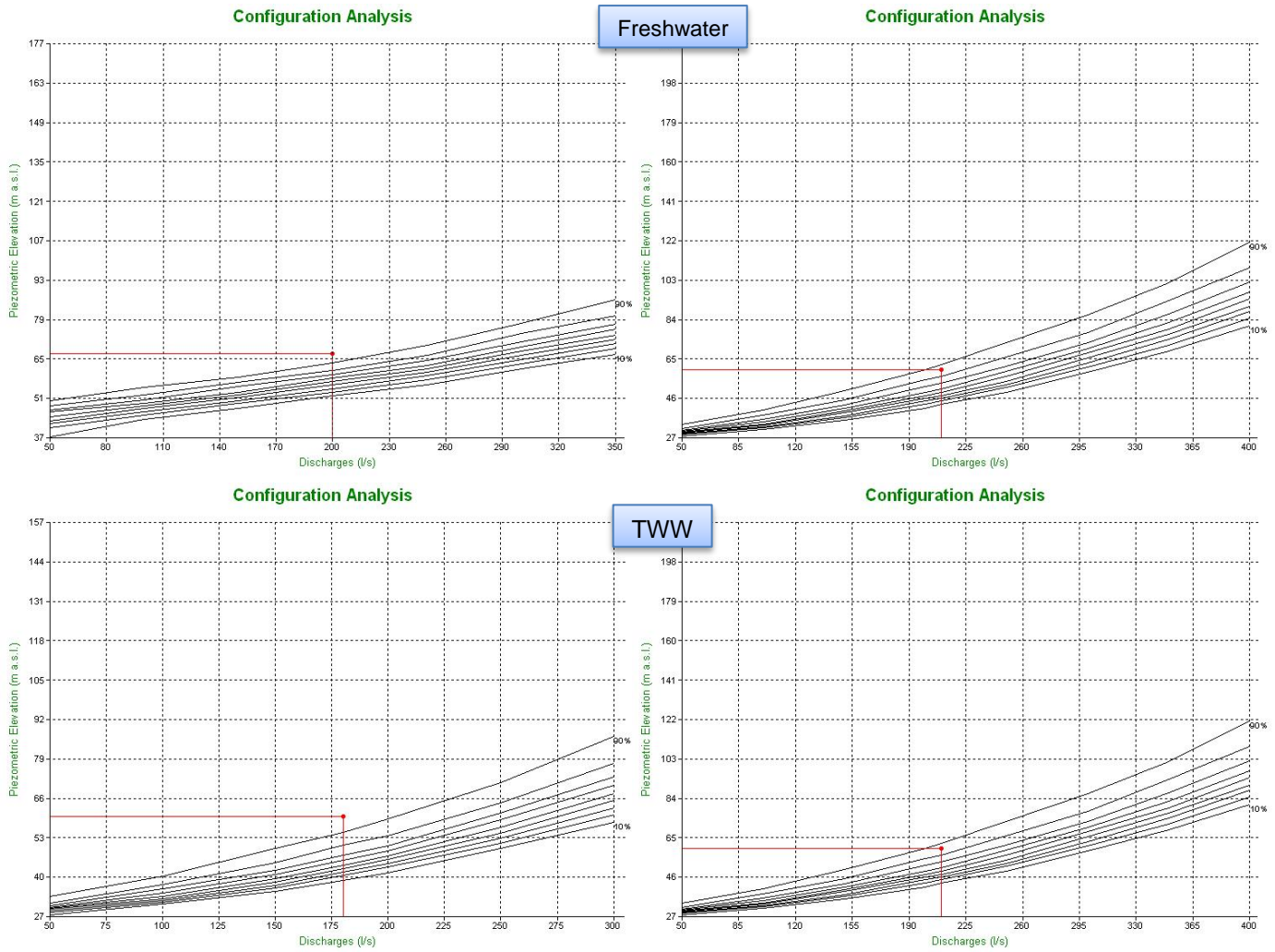


Fig. 19. Indexed characteristic curves for the average and dry year and sub-network 1 (freshwater) and sub-network 2 (TWW) generated by using 1000 random configurations.

Figure 20 shows the 100% pressure deficit curves. Table 12 demonstrates the number of hydrants per each pressure deficit class of the average year and the dry year. For 100% HPD, the number of hydrants included in the vacuum pressure class is 3 (1%) in the average year and 13 (4%) in the dry year. Regarding the pressure deficit between -1 to -0.2, there are 15 hydrants (5%) in the average year and 18 hydrants (6%) in the dry year. However, moving toward better pressure deficit classes, 14 hydrants (5%) are included in the pressure deficit class between -0.2 and 0 in the average year, and 11 hydrants (4%) in the dry year. When taking into account the good class between 0 and 5 pressure deficit, there are 278 hydrants (90%) in the average year, and 268 hydrants (86%) in the dry year, which are good percentage comparing the case before applying the deficit irrigation.

Freshwater

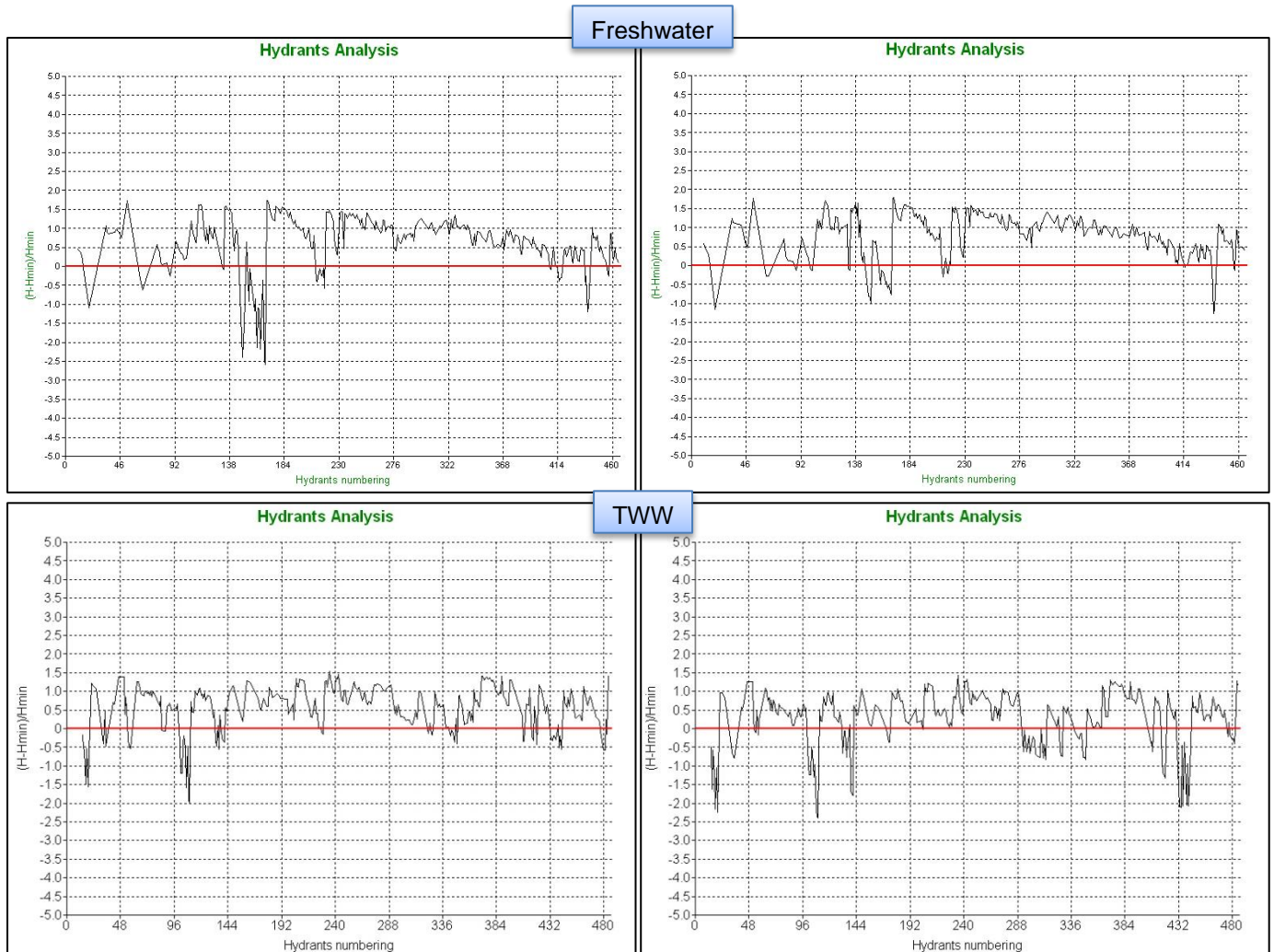






Fig. 20. The 100% pressure deficit curves for the average and dry year and sub-network 1 (freshwater) and sub-network 2 (TWW) generated by using 1000 random configurations.

For 90% HPD, it is noticeable that the number of hydrants subjected to vacuum pressure is zero in both, the average year and the dry year. When it comes to the pressure deficit between -1 and -0.2, there is only one hydrant in the average year, and 4 hydrants (4%) in the dry year. For the class from -0.2 to 0, only 2 hydrants (1%) are under deficiency in the average year and 3 hydrants (1%) in the dry year. The major part of the hydrants is included in the pressure deficit from 0 to 5, where there are 307 hydrants (99%) in the average year and 303 hydrants (98%) in the dry year. The state of the pressure deficit is much better when comparing the situation before using deficit irrigation. Additionally, there is a change in the system pressure deficit when the change from 100% to 90% pressure deficit, but the change is not that drastic. I mean, if 100% pressure deficit is considered to be the base for the analysis, some steps can be taken to improve the situation of low-performance hydrants, especially they are few, thus, can be controlled.

Table 12. The number and percentage of hydrants per each class of pressure deficit for the average and dry year and sub-network 1 (freshwater) and sub-network 2 (TWW).

Class	Bad	Poor	Fair	Good
Pressure deficit class				
	(-5) to (-1)	(-1) to (-0.2)	(-0.2) to (0)	(0) to (5)
Sub-network 1 (Freshwater)				
Average year				
100 % HPD	3.00	15.00	14.00	278.00
	1%	5%	5%	90%
90 % HPD	0.00	1.00	2.00	307.00
	0%	0%	1%	99%
Dry Year				
100 % HPD	13.00	18.00	11.00	268.00
	4%	6%	4%	86%
90 % HPD	0.00	4.00	3.00	303.00
	0%	1%	1%	98%
Sub-network 2 (TWW)				
Average year				
100 % HPD	7	35	19	257
	2%	11%	6%	81%
90 % HPD	0	0	6	312
	0%	0%	2%	98%
Dry year				
100 % HPD	23	47	15	233
	7%	15%	5%	73%
90 % HPD	0	10	6	302
	0%	3%	2%	95%

For TWW within 100% HPD, the number of hydrants within the vacuum pressure class is 7 (2%) in the average year and 23 (7%) in the dry. Concerning the pressure deficit from -1 to -0.2, there are 35 hydrants (11%) in the average year and 47 hydrants (15%) in the dry year. Nevertheless, keeping in view the pressure deficit between -0.2 and 0, there are 19 hydrants (6%) in the average year and 15 hydrants (5%) in the dry year. When taking into account the good class between 0 and 5 pressure deficit, there are 257 hydrants (81%) in the average year and 233 hydrants (73%) in the dry year. For 90% HPD, There are no hydrant experiencing pressure deficit between -1 and -0.2 in the average year, but 10 hydrants (3%) in the dry year. For the pressure deficit class from -0.2 to 0, only 6 hydrants (2%) are under deficiency in the average year and 6 hydrants (2%) in the dry year. The major part of the hydrants is within the pressure deficit from 0 to 5, where there are 312 hydrants (98%) in the average year and 302 hydrants (95%) in the dry year.

As can be noticed from Table 13, most of the hydrants are reliable indicating a reliable system. Going deeply into details, in both years, the average year and the dry year, the number of are few. Zero percent of hydrants have reliability of less than 0.5. Nevertheless, keeping in view the class 0.5 to 0.8, there is only 1 hydrant in the average year, and 4 hydrants in the dry year. 100% of hydrants in the average year have reliability from 0.8 to 1.0, while 99% of hydrants are in the same reliability class in the dry year. Table 13 confirms that 100% of the hydrants have reliability between 0.8 and 1 in the average year, while 99% of hydrants are in the same class in the dry year.

Table 13. The number and percentage of hydrants per each class of reliability for the average and dry year and sub-network 1 (freshwater) and sub-network 2 (TWW).




Class	Reliability indicator		
	Bad	Fair	Good
Pressure deficit class			
	<0.5	0.5-0.8	0.8-1.0
Sub-network 1 (Freshwater)			
Average Year	0	1	309
	0%	0%	100%
Dry year	0	4	306
	0%	1%	99%
Sub-network 2 (TWW)			
Average Year	0	0	318
	0%	0%	100%
Dry year	0	3	315
	0%	1%	99%

Figure 21 shows the GIS representation of a 100% pressure deficit of each hydrant for two years, the average year, and the dry year for sub-network 1. As it is shown in the maps, in the average year, few red-colored hydrants are having negative pressure, specifically in sectors 1 and 12. Yellow color hydrants present in sector 1 as well. The hydrants in green color are the dominant ones. The same situation appears in the dry year, except that the red and yellow hydrants increase in sector 1. Figure 22 presents the 90% pressure deficit of the average year and the dry year. It is obvious from the figure in both years that pressure deficit ranging from 0 to 5 is the dominant one, which indicates a high-performance system in case of a 90% pressure deficit.

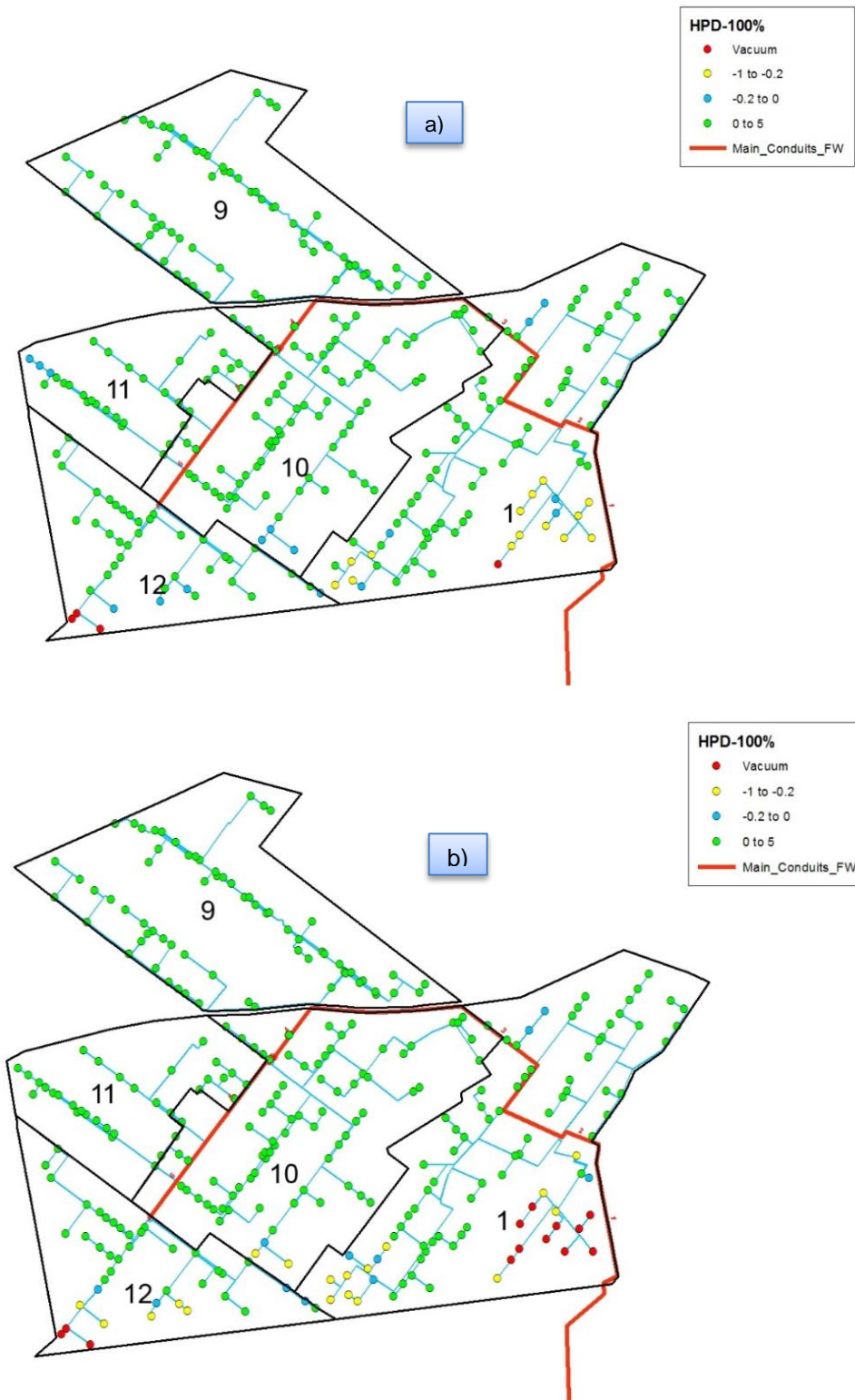


Fig. 21. GIS representation for 100% pressure deficit of each hydrant for sub-network 1. (a) Average year; (b) Dry year.

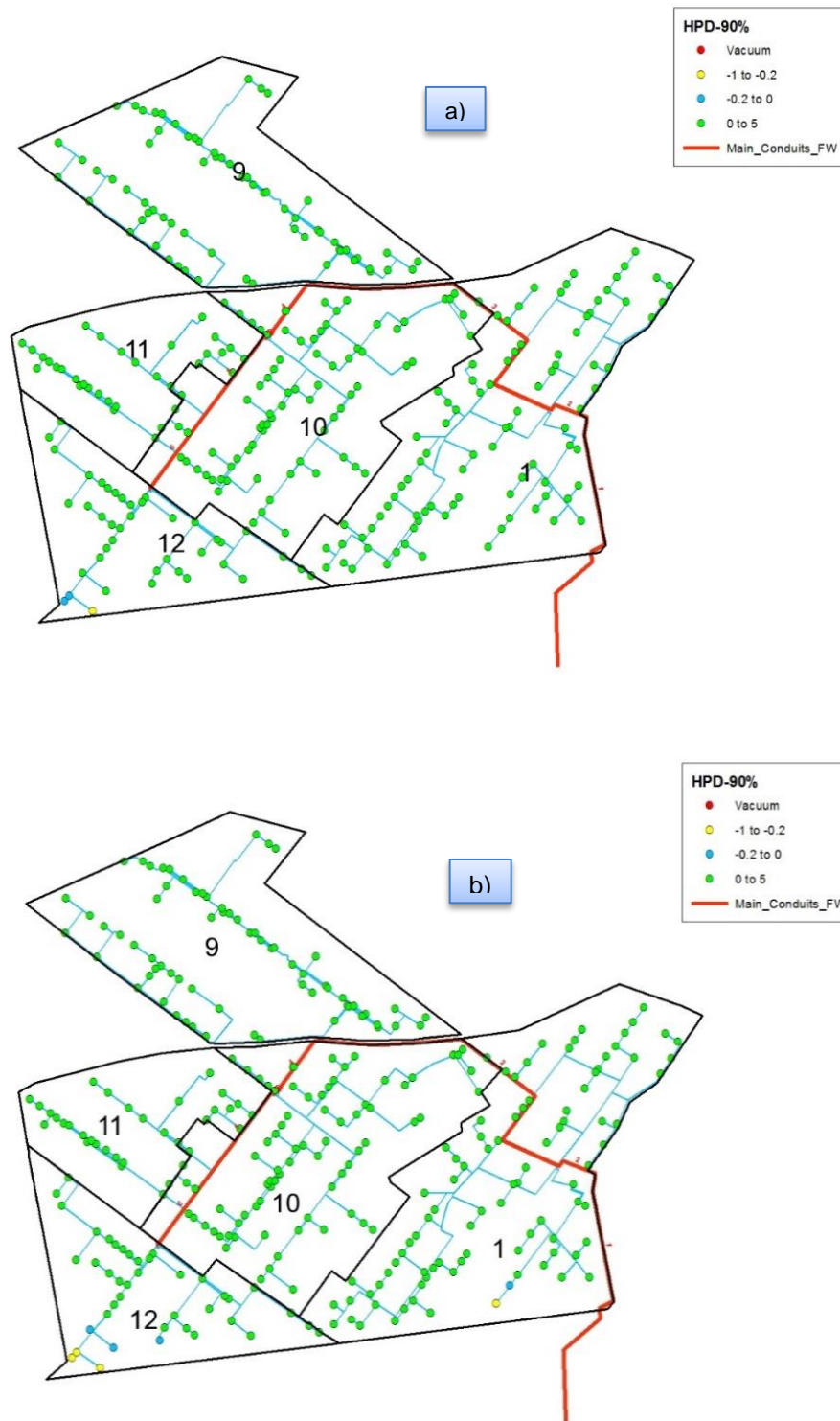


Fig. 22. GIS representation for 90% pressure deficit of each hydrant for sub-network 1. (a) Average year; (b) Dry year.

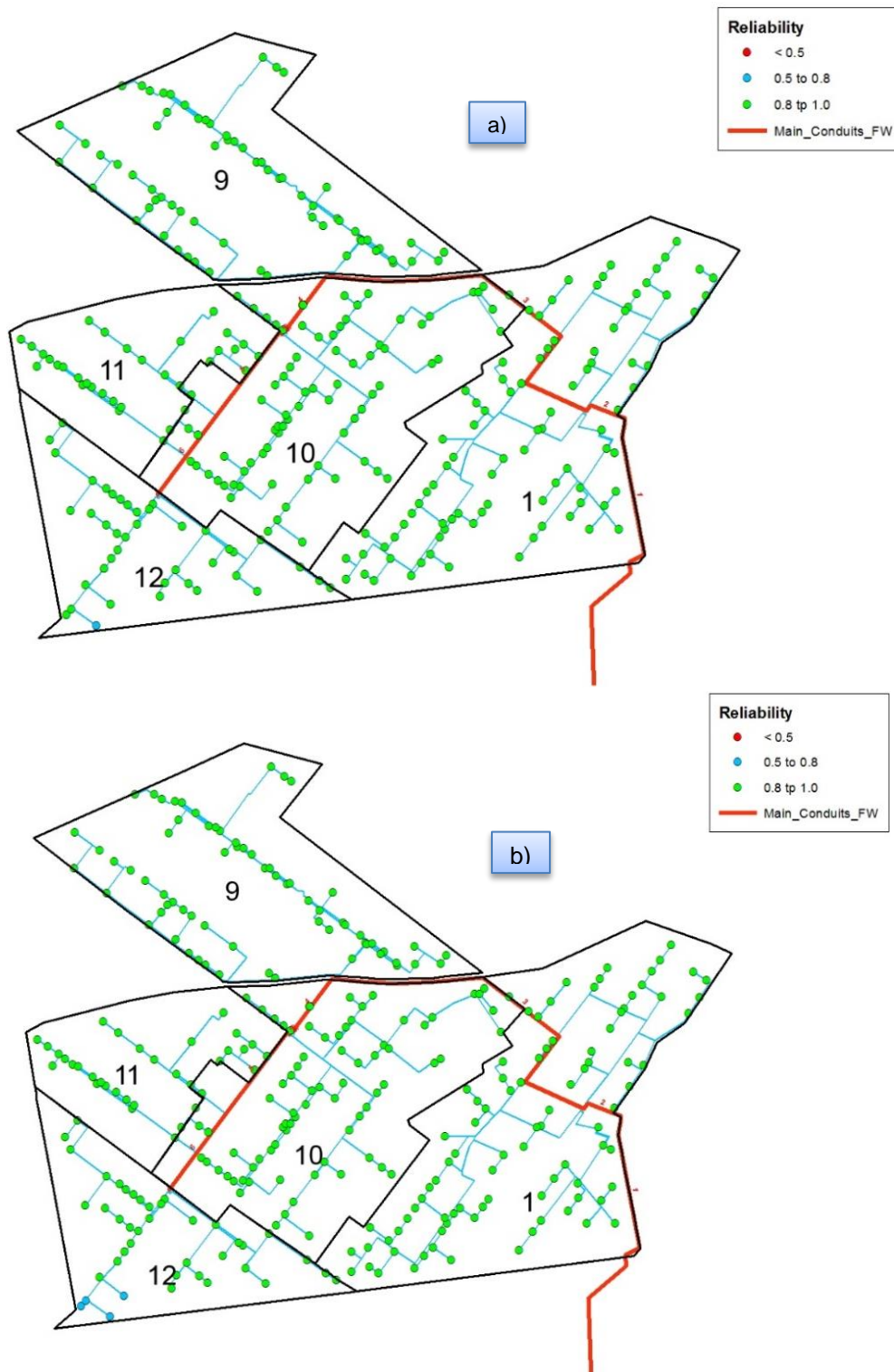


Fig. 23. GIS representation for the reliability of each hydrant for sub-network 1. (a) Average year (b) Dry year.



Fig. 24. GIS representation for 100% pressure deficit of each hydrant for sub-network 2. (a) Average year (b) Dry year.



Fig. 25. GIS representation for 90% pressure deficit of each hydrant for sub-network 2. (a) Average year (b) Dry year.

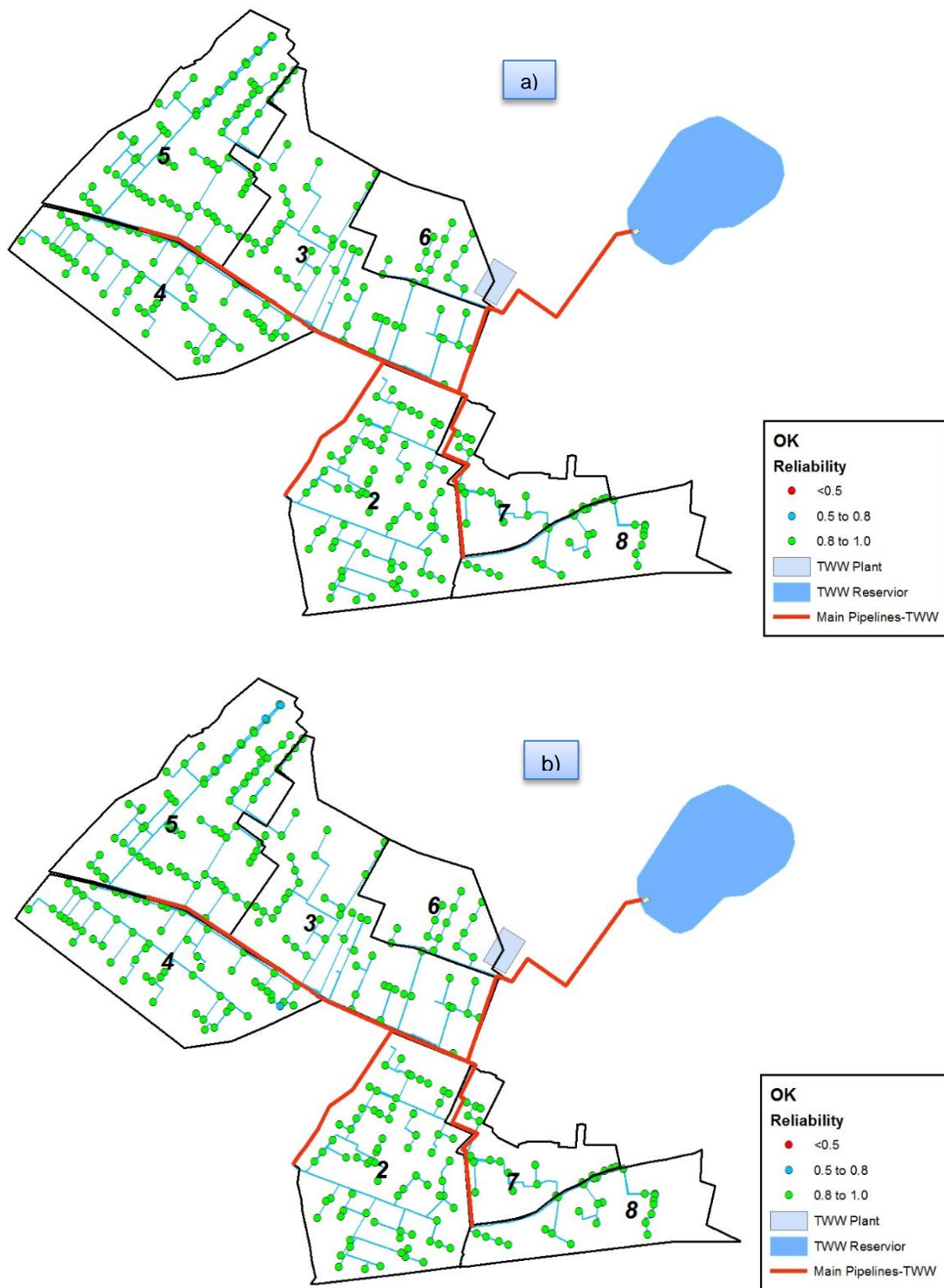


Fig. 26. GIS representation for the reliability of each hydrant for sub-network 2. (a) Average year (b) Dry year.

4. Concluding remarks

The implementation of performance analysis of an existing pressurized irrigation system operating on-demand has been examined with freshwater and wastewater sources and two climatic years, specifically, the average year and dry year. The performance analysis of an irrigation system with the use of simulation models was particularly useful to identify and quantify the operational problems in district 17 of the Sinistra Ofanto scheme (Southern Italy) as a case study. First, assuming all the district is irrigated by freshwater from the source. Second, share the total area between two sources of water (freshwater and TWW), where each source contributes irrigating 50% of the total area. For the first scenario, the results indicated low system performance using the average year, and much lower performance under dry year conditions. More specifically, the hydrant pressure deficit is distributed over all the networks, and the system was not enough reliable. In addition to that, the performance pointed out a vulnerable system when switching from 100% to 90% pressure deficit. The assessment of the district part irrigated by freshwater resulted in low performance of the system as well. To improve the performance of the freshwater part, deficit irrigation was applied for crops to reduce the system discharge keeping in consideration 90% of minimum crop yield. As a result, the system turned out to perform much better. Precisely, almost all hydrants are reliable in the two climatic years. Regarding the 100% pressure deficit, the major part of hydrants experienced a positive pressure deficit. Concerning the 90% pressure deficit, the situation was almost good for all hydrants. The change from 100% to 90% pressure deficit was smooth, which indicates a stable system. Similarly, the performance analysis of the district part irrigated by TWW also ended up with low operation performance of the system. Later, the same irrigation management was followed, which is to apply deficit irrigation but considering a minimum of 90% of crop yield. The deficit irrigation contributed to improving the performance of the TWW network part. All hydrants turned reliable for both climatic years. Besides, the 100% pressure deficit included some low-performance hydrants (e.g. 7 hydrants or 2% have pressure deficit between -5 to -1 in the average year, while there are 23 hydrants or 7% in the dry year having the same pressure deficit range). On the contrary, zero hydrants subjected to negative pressure for both climatic years, and 10 hydrants (3%) have a pressure deficit ranging from 1.0 to -0.2 in the dry year. The use of TWW for irrigation of crops would contribute to saving a good amount of water, and reduce the pressure on the freshwater source. Particularly, the TWW would help in saving about 498,000 Mm³ when considering the average year for the calculation of crop water requirements, and about 520, 000 Mm³ considering the dry year.

References

- D'Arcangelo, G., 2005. Non-Conventional Water Use in the Consorzio Di Bonifica of Capitanata (Apulia – Italy): Wastewater and Brackish Water. In : Hamdy A. (ed.), El Gamal F. (ed.), Lamaddalena N. (ed.), Bogliotti C. (ed.), Guelloubi R. (ed.). pp. 243–249.
- Dejen, Z. a., 2011. Hydraulic and Operational Performance of Irrigation System in View of Interventions for Water Saving and Sustainability, PhD Thesis.
- Derardja, B., Lamaddalena, N., Fratino, U., 2019. Perturbation indicators for on-demand pressurized irrigation systems. *Water (Switzerland)*. <https://doi.org/10.3390/w11030558>
- Fouial, A., Fernández García, I., Bragalli, C., Brath, A., Lamaddalena, N., Rodríguez Diaz, J.A., 2017. Optimal operation of pressurised irrigation distribution systems operating by gravity. *Agric. Water Manag.* <https://doi.org/10.1016/j.agwat.2017.01.010>
- Khadra, R., Lamaddalena, N., Inoubli, N., 2013. Optimization of on Demand Pressurized Irrigation Networks and On-farm Constraints. *Procedia Environ. Sci.* <https://doi.org/10.1016/j.proenv.2013.06.104>
- Lamaddalena, N., Lebdi, F., 2005. Diagnosis of pressurized irrigation systems in Lamaddalena N. (ed.), Lebdi F. (ed.), Todorovic M. (ed.), Bogliotti C. (ed.). *Irrigation systems performance*. Bari CIHEAM. Options Méditerranéennes Série B. Etudes Rech. 52, 9–22.
- Lamaddalena, N., Sagardoy, J., 2000. Performance analysis of on-demand pressurized irrigation. *Int. Cent. Adv. Mediterr. Agron. Stud.* 53, 1|. <https://doi.org/10.1017/CBO9781107415324.004>
- Levidow, L., Zaccaria, D., Maia, R., Vivas, E., Todorovic, M., Scardigno, A., 2014. Improving water-efficient irrigation: Prospects and difficulties of innovative practices. *Agric. Water Manag.* 146, 84–94. <https://doi.org/10.1016/j.agwat.2014.07.012>
- Polemio, M., 2016. Monitoring and management of karstic coastal groundwater in a changing environment (Southern Italy): A review of a regional experience. *Water (Switzerland)*. <https://doi.org/10.3390/w8040148>
- Smith, M., 1992. CROPWAT: A computer program for irrigation planning and management, FAO Irrigation and Drainage Paper 46.
- Stamouli, P., Dercas, N., Baltas, E., 2017. Performance analysis of on-demand pressurized irrigation networks – Case study in Greece 39–55.